

*Alma Mater Studiorum – Università di Bologna*

**DOTTORATO DI RICERCA IN**

**Medicina del Sonno**

**Ciclo XXII**

Settore scientifico-disciplinare di afferenza: MED / 26

**ADVANCED MR TECHNIQUES IN THE STUDY OF  
RESTLESS LEGS SYNDROME**

Presentata da: Dott. Giovanni Rizzo

**Coordinatore Dottorato**

**Relatore**

**Prof. Pasquale Montagna**

**Prof. Pasquale Montagna**

Esame finale anno 2010

*A mio padre*

*A Sara*

## CONTENTS

|   |    |
|---|----|
| INTRODUCTION .....  | 3  |
| Historical note .....   | 4  |
| Clinical features and diagnosis .....                           | 5  |
| Essential diagnostic criteria for RLS .....                     | 5  |
| Supportive clinical features of RLS .....                       | 6  |
| Associated features of RLS .....                                | 6  |
| Genetics .....  | 8  |
| Pathophysiology .....   | 9  |
| Central nervous structures and networks .....                   | 10 |
| Structural and microstructural abnormalities in MR studies..... | 11 |
| Dopaminergic system.....  | 12 |
| Iron metabolism .....   | 15 |
| OBJECTIVES .....  | 18 |
| METHODS .....   | 23 |
| Setting, timing and subjects .....                              | 24 |
| MR protocols.....   | 24 |
| RESULTS .....   | 31 |
| Structural and microstructural analysis.....                    | 32 |
| Subjects .....  | 32 |
| MR data.....  | 32 |
| <sup>1</sup> H-MRS.....   | 33 |
| Subjects .....  | 33 |
| MR data.....  | 33 |
| Phase imaging .....   | 33 |
| Subjects .....  | 33 |
| MR data.....  | 34 |
| DISCUSSION .....  | 35 |
| TABLES AND FIGURES .....  | 41 |
| REFERENCES.....   | 57 |

# **INTRODUCTION**

Restless legs syndrome (RLS) is the most common disorder of movement and quiet wakefulness, with a prevalence in the general population of 10–12% (with a range of 5–20% among different studies), that increases with age and is higher in women than in men (Trenkwalder C et al, 2005; Allen RP et al, 2003). It is characterised by an irresistible urge to move the legs, associated with unpleasant paraesthesias in the legs and sometimes in the arms. These sensations occur at rest, in particular in the evening or at night, and are relieved by movement. Many patients also have periodic limb movements in sleep (PLMS) and wakefulness (PLMW) and they may complain of insomnia and/or hypersomnia (Trenkwalder C et al, 2005; Allen RP et al, 2003). In the 70-80% of cases it is an idiopathic disorder with no apparent cause and in the remaining part is described as a symptomatic syndrome associated with pregnancy, uremia, iron depletion, polyneuropathy, spinal disorders, and rheumatoid arthritis (Bassetti C et al, 2001, Trenkwalder C et al, 2005), which is probably more correct to consider “risk factors” (Zucconi M, Ferini-Strambi L, 2004).

## **Historical note**

The first clinical description of restless legs is attributed to Thomas Willis, which described the syndrome in 1672 (Willis, 1685). In 1861 Wittmaack called the disorder "anxiety tibiaram," and wrote that it was a frequent symptom of hysteria (Wittmaack, 1861). Oppenheim was the first to define the disease as a neurologic illness and the first to recognize the genetic component of the disease (Oppenheim, 1923). The first significant clinical review of restless legs syndrome was written by Ekbom in 1945. He provided the basic modern description of the disorder and first suggested the currently accepted term “restless legs syndrome”. His monograph described 2 forms of the disorder: one form presents with prominent paresthesia, "asthenia crurum paresthetica," and the other form presents with prominent pain, "asthenia crurum dolorosa" (Ekbom, 1945). In 1953 Nils-Brage

Nordlander was the first to propose that iron deficiency may play a primary role in restless legs syndrome (RLS) (Nordlander NB, 1953). In 1953 Symonds described 5 patients with jerking of the extremities during sleep. He thought it could represent an epileptic disorder and called it "nocturnal myoclonus" (Symonds CP et al, 1953). In 1965, Lugaresi and colleagues first videopolysomnographically documented the presence of PLMS (adopting the Symonds' definition) in patients with RLS (Lugaresi E et al, 1965).

## **Clinical features and diagnosis**

In 1995, clinical diagnostic criteria for the restless legs syndrome were established by the International Restless Legs Syndrome Study Group (IRLSSG) (Walters AS, 1995), and reviewed in 2003 (Allen RP et al, 2003). These include four essential criteria that all must be met and three supportive criteria. Furthermore additional significant clinical features are associated with the disorder.

### ***Essential diagnostic criteria for RLS***

- 1) An urge to move the legs, usually accompanied or caused by uncomfortable and unpleasant sensations in the legs (Sometimes the urge to move is present without the uncomfortable sensations and sometimes the arms or other body parts are involved in addition to the legs)
- 2) The urge to move or unpleasant sensations begin or worsen during periods of rest or inactivity such as lying or sitting
- 3) The urge to move or unpleasant sensations are partially or totally relieved by movement, such as walking or stretching, at least as long as the activity continues

- 4) The urge to move or unpleasant sensations are worse in the evening or night than during the day or only occur in the evening or night (When symptoms are very severe, the worsening at night may not be noticeable but must have been previously present)

### ***Supportive clinical features of RLS***

- 1) Family history: the prevalence of RLS among first-degree relatives of people with RLS is 3 to 5 times greater than in people without RLS.
- 2) Response to dopaminergic therapy: nearly all people with RLS show at least an initial positive therapeutic response to either L-dopa or a dopamine-receptor agonist at doses considered to be very low in relation to the traditional doses of these medications used for the treatment of Parkinson disease. This initial response is not, however, universally maintained.
- 3) Periodic limb movements (during wakefulness or sleep): periodic limb movements in sleep (PLMS) occur in at least 85% of people with RLS; however, PLMS also commonly occur in other disorders and in the elderly. In children, PLMS are much less common than in adults.

### ***Associated features of RLS***

- 1) Natural clinical course: the clinical course of the disorder varies considerably, but certain patterns have been identified that may be helpful to the experienced clinician. When the age of onset of RLS symptoms is less than 50 years, the onset is often more insidious; when the age of onset is greater than 50 years, the symptoms often occur more abruptly and more severely. In some patients, RLS can be intermittent and may spontaneously remit for many years.
- 2) Sleep disturbance: disturbed sleep is a common major morbidity for RLS and deserves special consideration in planning treatment. This

morbidity is often the primary reason the patient seeks medical attention.

- 3) Medical evaluation/physical examination: the physical examination is generally normal and does not contribute to the diagnosis except for those conditions that may be comorbid or secondary causes of RLS. Iron status, in particular, should be evaluated because decreased iron stores are a significant potential risk factor that can be treated. The presence of peripheral neuropathy and radiculopathy should also be determined because these conditions have a possible, although uncertain, association and may require different treatment.

In summary RLS is a sensorimotor disorder. The sensory components include discomfort in the legs with an urge to move that patients report using different and sometimes bizarre descriptions: creepy-crawly, ants crawling, jittery, pulling, worms moving, soda bubbling in the veins, electric current, shock-like feelings, pain, the gotta moves, burning, jimmy legs, heebie jeebies, tearing, throbbing, tight feeling, grabbing sensation, elvis legs, itching bones, crazy legs, fidgets (Walters AS, 1996). The motor component is characterized by the need to walk and involuntary periodic leg movements during wakefulness (PLMW) and during sleep (PLMS).

In the diagnostic process particular attention must be made in order to exclude other conditions that may resemble RLS. Indeed, an interview with a trained physician is necessary for the correct diagnosis of RLS: if only questionnaires with the RLS criteria are given to patients this results in approximately 10–25 % false positives due to the so-called “RLS mimics”, which include akathisia, nocturnal leg cramps, peripheral neuropathy, lumbosacral radiculopathy, painful legs and moving toes, growing pains, attention deficit hyperactivity disorder (ADHD) (Hening WA et al, 2009).

Useful diagnostic tool is the suggested immobilization test (SIT), that evaluates periodic leg movements (PLM) and self-reported sensory symptoms for people who are instructed to remain still for 1 h while sitting on a bed with their legs outstretched (Michaud M et al, 2002).

Polysomnography allows accurate assessment of PLMS, scoring them only if they occur in a series of four consecutive movements lasting 0.5-5 s, have an amplitude of one quarter or more of the toe dorsiflexion during calibration and are separated by intervals of 4-90 s. They occur during the stages 1-2 of NREM sleep, diminish during stages 3-4 and nearly always disappear during REM sleep. An index (number of PLMS per hours of sleep) greater than 5 for the entire night is considered pathologic and is supportive, although not specific, of the diagnosis of RLS (Zucconi M et al, 2006). The PLMW, both during the sleep period and the SIT, appear to be more specific for RLS, but the data for this finding remain limited (Montplaisir J, et al, 1998; Nicolas A et al, 1999).

With regard to the quantification of RLS symptoms, since it is primarily a subjective disorder, a subjective scale represents the optimal instrument to measure disease severity for clinical assessment, research, or therapeutic trials. Therefore, in 2003 the IRLSSG proposed and validated a rating scale, consists of ten questions, whose total score progresses from 0 to 40 with the degree of disease severity (Walters AS et al, 2003).

## **Genetics**

A family history of RLS is present in more than 50% of affected individuals (Zucconi M, Ferini-Strambi L, 2004). RLS is 3-5 times greater amongst first degree relatives of subjects suffering from RLS than in subjects without RLS (Allen RP et al, 2003) and pedigrees mostly suggest an autosomal-dominant transmission with high penetrance. The possibility of anticipation has been described (Trenkwalder C et al, 1996; Lazzarini A et al, 1999). Variations in penetrance and anticipation suggest possible genetic heterogeneity (Lazzarini A et al, 1999). RLS has also been reported to have a high concordance for monozygotic (61%) and dyzygotic twins (45%) (Desai AV et al, 2004). Clinically, familial forms cannot be differentiated from sporadic or symptomatic forms (Winkelmann J et al, 2000) except for

an earlier age of onset and a more slowly progressive course in familial cases (Allen RP and Earley CJ, 2000; Winkelmann J et al, 2002).

Linkage analysis actually have detected nine gene loci associated to familial forms of RLS (RLS1-9), located on chromosomes 12q, 14q, 9q, 2q, 20p, 4q, 17p, 19p, 16p, all autosomal-dominant except the first one that is recessive (Trenkwalder C et al, 2009; Levchenko A et al, 2009), but no candidate gene has been identified. On the basis of knowledge of the pathophysiology of RLS (see below) some candidate genes have been studied - i.e. those coding for D1–D5 receptors, DAT, TH, Dopamine  $\beta$  hydroxylase, GTP cyclohydrolase, GABA A receptor subunits ( $\alpha$ 1-6,  $\beta$  1-3,  $\chi$ 1-3, p1-2),  $\alpha$ -1 subunit of the glycine receptor (chromosome 5q31), MAO-A, MAO-B, Neurotensin – without disclosing any mutation or clearly predisposing polymorphism (Winkelmann J et al, 2007a; Dhawan V et al, 2006).

Recently, a genome-wide case-control study of single-nucleotide-polymorphisms (SNPs) has showed association between RLS and three genetic loci: one within *MEIS1*, one within *BTBD9* and one between *MAP2K5* and *LBXCOR1* (Winkelmann J et al, 2007b). Another genome-wide association study of RLS and PLM reported association with one of these genes, *BTBD9* (Stefansson H et al, 2007). All these genes have been implicated in development mechanisms, raising the possibility that RLS has components of a developmental disorder. Interestingly *BTBD9* also affects ferritin level and iron storage (Mignot E, 2007).

## **Pathophysiology**

The pathophysiology of RLS is poorly understood. A lot of observations point towards an involvement of central nervous structures and networks, dopaminergic system and iron metabolism.

### ***Central nervous structures and networks***

RLS dysfunction appears to involve the central nervous system, but the areas involved are somewhat uncertain. Functional MRI (fMRI) demonstrated an activation of the thalamus (legs discomfort), cerebellum (legs discomfort and PLM), red nuclei and brainstem (PLM) (Bucher SF et al, 1997). A more recent fMRI study, using only a motor paradigm, found activation in the thalamus, the putamen, the middle frontal gyrus and the cingulate gyrus (Astrakas LG et al, 2008).

Electrophysiological studies suggest that the movements are involuntary and are organized at the brainstem or spinal level (Trenkwalder C et al, 1996). Patients with periodic leg movements of sleep, with or without associated restless legs syndrome, may have abnormal blink reflexes (Briellmann RS et al, 1996). H-reflexes with its modulation (Martinelli p and Coccagna G, 1976; Rijsman RM et al, 2005; Scaglione et al 2008) and flexor reflex (Bara-Jimenez W et al, 2000) are impaired suggesting a brainstem or more rostral dysfunction leading to enhanced spinal excitability. Cortical prepotentials associated with the PLMS or PLMW have generally not been found (Lugaresi et al, 1986; Trenkwalder et al, 1993). Recently a study disclosed that in RLS patients the event-related beta and mu (de)synchronization amplitudes and durations for voluntary movement were greater during the symptomatic period (at 8:30 PM) than during the asymptomatic (at 8:30 AM) period and in comparison with healthy controls, suggesting the presence of cortical sensorimotor dysfunction (Tyvaert L et al, 2009a). Cortical transcranial magnetic stimulation (TMS) studies in RLS show that the pyramidal tract is intact, whereas the excitatory and inhibitory system seems to be altered, but can be influenced and restored by treatment with dopamine-agonists (Nardone R et al, 2006; Kutukcu Y et al, 2006; Gorsler and Liepert, 2007; Rizzo V et al, 2009).

All these studies are consistent with a subcortical dysfunction that alters function of the motor pathways.

Clinical observations in patients after an ischemic stroke suggest that lesions of the subcortical brain areas such as the pyramidal tract, thalamus and the basal ganglia-brainstem axis, which are involved in motor functions and sleep-wake cycles, may lead to RLS symptoms (Lee SJ et al, 2009; Unrath A et al, 2006). A study in patients with multiple sclerosis disclosed a higher prevalence of RLS associated to greater cervical cord damage and speculated about a possible brain-spinal disconnection (Manconi M et al, 2008).

Therefore, RLS appears as a complex movement disorder affecting several levels of the neuraxis, even though the precise pathoanatomic location of this dysfunction has not yet been determined (Barrière G et al, 2005). However, there is evidence for impairment of sensorimotor processing at the level of the cortex and the spinal cord, suggesting altered subcortical/supraspinal control.

### ***Structural and microstructural abnormalities in MR studies***

Conventional cranial MRI does not identify any structural abnormalities in RLS patients. MR studies using advanced techniques reported contrasting data. A voxel based morphometry (VBM) study detected a bilateral gray matter increase in the pulvinar and the authors assumed that these changes in thalamic structures may reflect a consequence of chronic increase in afferent input of behaviourally relevant information (Etgen T et al, 2005). Successive VBM studies did not confirm this result, but one disclosed significant regional decreases of gray matter volume in the bihemispheric primary somatosensory cortex, which additionally extended into left-sided primary motor areas (Unrath A et al, 2007), another one slightly increased gray matter density in the ventral hippocampus and in the middle orbitofrontal gyrus (Hornyak M et al, 2007), and yet another one lack of specific gray matter alterations (Celle S et al, 2009).

Only one diffusion tensor imaging (DTI) study of RLS is present in literature (Unrath A et al, 2008). In the patient group, multiple subcortical

areas of significantly reduced fractional anisotropy (FA) (a quantitative marker of white matter integrity) were observed bihemispherically in close proximity to the primary and associate motor and somatosensory cortices, in the right-hemispheric thalamus (posterior ventral lateral nucleus), in motor projectional fibers and adjacent to the left anterior cingulum. The authors suggested that these findings gave support to an altered subcortical network, with the major component of altered cerebral sensorimotor pathways, within a hodological concept of the RLS pathoanatomy (Unrath A et al, 2008).

Despite these conflicting data the investigation about structural abnormalities in RLS remains an actual point of interest, also in light of the discovery of a possible role of genes involved in development mechanisms (*MEIS1*, *BTBD9*, *MAP2K5* and *LBXCOR1*) (Winkelmann J et al, 2007b).

### ***Dopaminergic system***

The dopaminergic system involvement is highly probable because treatment with dopamine agonists shows efficacy as confirmed by controlled trials, while dopamine antagonists worsen symptoms or may even elicit RLS (Barrière G et al, 2005). Many studies reported an increased prevalence of RLS in PD patients, although they are difficult to interpret because the current diagnostic criteria for RLS have not been validated in PD patients and “RLS mimics” could have been affect the results (Möller JC et al, 2010). PET and SPECT studies revealed some controversial results of the pre- and postsynaptic dopaminergic neurotransmission system. Almost all have focused on the striatum, a brain region receiving dense dopaminergic innervations, showing slight reduction binding or no difference of both presynaptic ( $[^{123}\text{I}]\beta\text{CIT}$ ,  $[^{123}\text{I}]\text{IPT}$  or  $[^{99\text{m}}\text{Tc}]\text{TRODAT-1}$  in SPECT studies and  $^{18}\text{F}$ -dopa in PET studies) and postsynaptic D2 radioligand ( $[^{123}\text{I}]\text{IBZM}$  in SPECT studies and  $^{11}\text{C}$ -raclopride in PET studies) in RLS patients when compared with control subjects (Wetter TC et al, 2004; Hilker R et al, 2006). Taken together, these results suggest that at level of nigro-striatal pathway the membrane dopamine transporter and postsynaptic D2-receptor

seem to be either unchanged or mildly reduced in patients with idiopathic RLS. The most recent PET study investigated, besides striatal regions by  $^{11}\text{C}$ -raclopride, other extrastriatal dopaminergic regions by FLB 457 (a new postsynaptic high-affinity D2 radioligand) and disclosed a higher binding potential in patients than controls at level of limbic and associative part of striatum, medial and posterior part of thalamus, anterior cingulate cortex and insule, all part of the medial nociceptive system which is thought to regulate the affective-motivational component of pain. The authors sustained the hypothesis of hypoactive dopaminergic neurotransmission associated to receptor up-regulations (Cervenka S et al, 2006). An involvement of the medial nociceptive system was supported also by a PET with [ $^{11}\text{C}$ ]diprenorphine, a non-selective opioid receptor radioligand, which found regional negative correlations between ligand binding and RLS severity in areas serving the medial pain system (medial thalamus, amygdala, caudate nucleus, anterior cingulate gyrus, insular cortex and orbitofrontal cortex) (von Spiczak S et al, 2005).

In a recent pathological study, the substantia nigra and putamen were obtained at autopsy from individuals with primary RLS and a neurologically normal control group and a quantitative profile of the dopaminergic system was obtained. RLS tissue, compared with controls, showed a significant decrease in D2R in the putamen that correlated with severity of the RLS. RLS also showed significant increases in tyrosine hydroxylase (TH) in the substantia nigra, compared with the controls but not in the putamen, and both with the decrease of D2R, interpreted as a down-regulation, led authors to hypothesize an overly activated dopaminergic system as possible part of the RLS pathology (Connor JR et al, 2009). The hypothesis of an increase in dopamine activity and turnover is consistent with the recent CSF studies showing increased 3-Ortho-methyldopa (3OMD) in RLS patients off dopamine treatment that correlates well with increased HVA (Allen et al, 2008).

These contrasting data could be explained by the difference in the methodologies and in selected patients (mild o severe RLS). However, even

if cerebral metabolism in RLS probably reflects a dysfunction of the central dopaminergic system, it has still to be determined whether these alterations affect mainly the nigrostriatal and/or other central dopaminergic systems like the diencephalospinal or mesolimbic pathway and whether they are the primary mechanisms or only secondary phenomena within the manifestation of RLS symptoms.

In the last years great interest has developed around the involvement of diencephalospinal pathway in RLS. Some authors forward the hypothesis that RLS reflects a dysfunction of the little-studied dorso-posterior hypothalamic dopaminergic A11 cell group (Clemens S et al, 2006). The A11 cell group in the dorso-posterior hypothalamus and subparafascicular thalamus is the largest, possible sole, source of spinal DA (Skagerberg G et al, 1982 and 1985; Qu S et al, 2006). A11 spinal projections innervate all of Rexed's laminae and are most heavily concentrated in the superficial sensory-related dorsal horn and the intermediolateral nucleus (IML). They modulate sensory inputs and sympathetic drive, predominantly with inhibitory action through D2 and especially D3 receptors (Clemens S et al, 2006). This theory was supported from some animal models which disclosed that D3 receptor knockout (D3KO) mice are hyperactive and manifest an increased wakefulness across the rest-activity cycle (Accili D et al, 1996; Hue GE et al, 2003) and that locomotor activities were significantly increased in A11-lesioned mice compared with controls (Ondo WG et al, 2000; Qu S et al, 2007). A recent neuropathological study shows no evidence of changes in the number and volume of TH (+) neurons, neither atrophy nor hypertrophy nor gliosis in the A11 region in the posterior hypothalamus of RLS patients compared with age-matched control cases (Earley CJ et al, 2009). These results could support a functional involvement rather than a degeneration of A11 region.

### ***Iron metabolism***

The potential central role of iron metabolism involvement in RLS is indicated primarily by those secondary forms of RLS in which iron insufficiency is clear, but also from some limited pharmacological studies which demonstrated that by using intravenous or oral iron, one could markedly improve, if not resolve, RLS symptoms, even in those who apparently had normal blood levels of iron (Nordlander NB, 1953; Earley CJ et al, 2005; Wang J et al, 2009). Several studies showed a relation between low ferritin concentrations and symptoms of the syndrome, especially when ferritin was measured in the cerebrospinal fluid (CSF). This link to the iron deficiency is particularly strong for early-onset RLS (Clardy SL et al, 2006a). Studies on CSF showed decreased ferritin, elevated transferrin and decreased pro-hepcidin (that interacts with the iron transport protein ferroportin on the surface of cells) in patients with RLS (Clardy SL et al, 2006b). Neuropathological studies found alterations of iron regulatory proteins (decreased ferritin, divalent metal transporter 1, ferroportin, transferrin receptor and increased hepcidin) in neuromelanin cells from brains of patients (Connor JR et al, 2003 and 2004). Altered iron metabolism was disclosed in lymphocytes from subjects with RLS (Earley CJ et al, 2008). A recent pathological study showed that RLS substantia nigra had more mitochondrial ferritin levels and less cytosolic H-ferritin than control samples (Snyder AM et al, 2009). Reduced brain iron in RLS patients is also suggested by the data of some MR studies that exploit the effect of iron on T2, T2\* and T2' (and associate parameters R2, R2\* and R2'), although with discrepant results. It has been well documented through in vitro studies that paramagnetic iron will increase proportionally proton transverse relaxation rates ( $R_2=1/T_2$ ). Furthermore, ferritin and hemosiderin are considered to be the only forms of nonheme iron present in sufficient quantities to affect MR contrast in the human brain (Haacke EM et al, 2005). In two studies of the same group regional brain iron concentration were assessed in RLS patients by  $R_2'$  measurement, and the mean iron content from the substantia nigra was significantly lower in the early-onset

RLS patients (< 45 years) and not in the late-onset (Allen RP et al, 2001; Earley CJ et al, 2006). In a study performed in patients with late-onset RLS, the T2 relaxation time was assessed separately for the two components of the SN, and low iron content was found in the SN pars compacta (and not in the pars reticulata) (Astrakas LG et al, 2008). Another group, without differentiating between early-onset and late-onset, disclosed that mean T2 values of multiple regions were higher in RLS patients, though significantly increased only in four regions (caudate head, thalamus medial, dorsal and ventral); the mean T2 over all voxels was higher in patients, indicating a multiregional (global) brain iron deficiency in RLS patients (Godau J et al, 2008). Also transcranial B-Mode sonography was used in RLS patients which exhibited substantia nigra hypoechogenicity correlated inversely with T2 values and interpreted as related to iron deficiency (Schmidauer C et al, 2005; Godau J et al, 2008).

These observations has led to a more general iron-dopamine model of RLS and it has been suggested that dopaminergic dysfunction can be mediated by low brain iron levels since iron is needed as a cofactor for tyrosine hydroxylase (the rate limiting enzyme in the synthesis of dopamine), because the D<sub>2</sub> receptor is a protein containing iron, and because the dopaminergic synaptic protein Thy-1 requires iron for its activity. Hence a brain iron deficiency could lead to lowering dopamine production via reduced tyrosine hydroxylase activity, down-regulation of dopamine type 2 receptors and destabilization of dopaminergic synapses (Allen RP, 2004; Allen RP and Earley CJ, 2007).

In support of this hypothesis there are some animal models which reported increase of wakefulness in the 4 hours preceding the resting phase of iron-deficient mice (Dean T et al, 2006), increased locomotor activities in the mice that were iron deprived, with a further significantly augmented activity after combination of iron deprivation and A11 lesions (Qu S et al, 2007), increased locomotor activities in the mice treated with iron-deficiency diet (ID), which were reversed by the D2/D3 agonist ropinirole, and a

synergistic greater decrease of spinal cord D2 binding in mice underwent both ID and 6-OHDA lesion of A11 region (Zhao H et al, 2007).

Finally *BTBD9* gene recently associated to RLS and PLM, affects ferritin level and iron storage (Winkelmann J et al, 2007b; Stefansson H et al, 2007; Mignot E, 2007).

## **OBJECTIVES**

This study was designed to evaluate RLS patients by multiple advanced MR techniques in order to investigate three different aspects of the pathophysiology of the disease:

- 1) To evaluate the presence of structural and/or microstructural abnormalities in the brain of RLS patients using voxel-based morphometry (VBM) and diffusion tensor imaging (DTI) analysis, considering the contradictory data reported in previous studies (Etgen T et al, 2005; Hornyak M et al, 2007; Celle S et al, 2009; Unrath A et al, 2007 and 2008).
- 2) To investigate metabolic functions of the thalamus of RLS patients using proton magnetic resonance spectroscopy (<sup>1</sup>H-MRS), considering the possible involvement of this structure disclosed by MRI (Bucher SF et al, 1997; Astrakas LG et al, 2008; Lee SJ et al, 2009; Unrath A et al, 2006) and PET studies (Cervenka S et al, 2006; von Spiczak S et al, 2005).
- 3) To evaluate brain iron content in RLS patients using phase imaging. The primary hypothesis was that patients have low whole-brain iron levels. Additionally certain regions previously suspected of low iron concentrations were assessed separately (Allen RP et al, 2001; Earley CJ et al, 2006; Astrakas LG et al, 2008; Godau J et al, 2008).

## **VBM**

VBM is an automated technique that assesses patterns of regional atrophy on MRI between groups of subjects. Mainly and more accurately it investigates voxel-wise changes in the grey matter volume/topography rather than white matter. The procedure is relatively straightforward and involves spatially normalizing high-resolution images from all the subjects in the study into the same stereotactic space. This is followed by segmenting the gray matter from the spatially normalized images and smoothing the gray-matter segments. Voxel-wise parametric statistical tests which compare the smoothed gray-matter images from the groups are performed.

Corrections for multiple comparisons are made using the theory of Gaussian random fields (Ashburner J and Friston K, 2000). It is unbiased in that it looks throughout the whole brain and does not require any a priori assumptions concerning which structures to assess. This gives it a significant advantage over more traditional region of interest (ROI) based methods, which typically involve drawing around a structure of interest.

## **DTI**

Diffusion tensor imaging (DTI) is sensitive to water diffusion characteristics (such as the principal diffusion direction and the diffusion anisotropy) and has therefore been developed as a tool for investigating the local properties and integrity of brain tissues, mainly at level of white matter tracts but also at level of grey matter (Pierpaoli P et al, 1996). Post-processing of the acquisitions allows the reconstruction of maps of the mean diffusivity (MD) and of the white matter anisotropic properties, usually in terms of fractional anisotropy (FA) (Mascalchi M et al, 2005). Neuronal and/or axonal loss is typically characterised by increased MD and reduced FA, as modification of brain tissue integrity reduces the barriers that restrict the movement of water (Rizzo G et al, 2008; Agosta F et al, 2009). Maps of MD and FA may be analysed using a ROIs approach to evaluate single structures, using a histogram approach to evaluate greater portions of the brain or whole brain and using voxel-wise analyses for an unbiased approach. We utilised all three approaches. For the voxel-wise analyses we used tract-based spatial statistics (TBSS), which aims to solve crucial issues of cross-subject data alignment, allowing localized cross-subject statistical analysis (avoiding the arbitrariness of the choice of spatial smoothing extent), using the “mean FA skeleton” approach (Smith SM et al, 2006 and 2007).

## **<sup>1</sup>H-MRS**

Magnetic resonance spectroscopy (MRS) is a noninvasive method that permits measurement of the concentration of specific biochemical compounds in the brain and other organ systems in precisely defined regions

guided by MR imaging. With MR spectroscopy we can measure spectra of many biologically interesting isotopes. In vivo biomedical applications are mainly focused on proton ( $^1\text{H}$ ), phosphorus ( $^{31}\text{P}$ ) and carbon ( $^{13}\text{C}$ ) isotopes (Hajek M et al, 2008). The most used in clinical practice is  $^1\text{H}$  MRS. At long echo-time (TE)  $^1\text{H}$  MRS can detect N-acetyl-aspartate containing compounds, choline containing compounds, creatine-phosphocreatine and lactate. At short TE, lipids, triglycerides, glutamate, glutamine, scyllo-inositol, glucose, myo-inositol, are visible (Bonavita S et al, 1999). The most relevant metabolites in neurological studies are probably N-acetyl-aspartate (NAA), a neuronal marker (Kantarci K et al, 2008), and myo-inositol (mI) a glial marker (Brand A et al, 1993).  $^1\text{H}$  MRS can be performed with single-voxel, multivoxel, single slice and multislice techniques. This technique can be useful in the study a number of central nervous system disorders such as epilepsy, brain tumors, stroke, multiple sclerosis, degenerative disorders (identification of microscopic pathology not visible with MRI) and metabolic diseases (metabolic disturbances with specific metabolic patterns) (Lodi R et al, 2009; Bonavita S et al, 1999).

## **Phase imaging**

This is a new neuroimaging technique (a part of susceptibility-weighted imaging, SWI), which uses tissue magnetic susceptibility differences to generate a unique contrast, different from that of spin density, T1, T2, and T2\* (Haacke EM et al, 2009). It measures the phase shifts in gradient-echo images. It seems a very sensitive tool to quantify the iron content of the brain (Ogg RJ et al, 1999). Furthermore, while R1 ( $1/\text{T1}$ ) and R2 ( $1/\text{T2}$ ) can be reversible depending on the water content and other local structural changes that can affect relaxation times (in these cases, the effect of iron remains invisible), this is not true for R2' ( $\text{R2}'=\text{R2}^*-\text{R2}$ ) or phase (Haacke EM et al, 2005). Tissue containing (paramagnetic) iron exhibits a negative phase in complex images compared to immediately adjacent tissue, which will have an increased phase. Phase imaging allows a qualitative evaluation based on the unique contrast resulting in the images and a quantitative

analysis based on the evaluation of local phase differences (measured in radians).

## **METHODS**

## **Setting, timing and subjects**

A total of 25 patients (age  $52\pm 10$ , mean  $\pm$  SD; 10 males and 15 females) (**Table 1**) were recruited by Sleep Medicine Centre of the Department of Neurological Science of Bologna University and they were studied by MR in the MR Spectroscopy Unit of the Department of Internal Medicine, Aging and Nephrology of Bologna University, from January 2007 to May 2009. The patients will satisfy the revised criteria of IRLSSG (Allen RP et al, 2003). Secondary forms of RLS were excluded by exploring a detailed history, by objective evaluation and using laboratory analyses such as hemoglobin, iron, ferritin, transferrin, creatinine, urea and liver enzymes. The severity of RLS was assessed on the day of scan using the IRLSSG rating scale (Walters AS et al, 2003).

We have studied also 22 healthy control subjects (age  $49\pm 16$ , mean  $\pm$  SD; 14 males and 8 females).

All control subjects were interviewed by a Sleep Medicine expert in order to exclude symptoms suggesting RLS and other neurological disorders. Both patients and controls gave written informed consent. Both patients and controls not always underwent the complete MR protocol because of time or technical problems. So the studied samples differ among the different protocols.

## **MR protocols**

Subjects were studied in a 1.5 Tesla GE Signa Horizon LX system equipped with a birdcage head radio-frequency coil for signal reception and an EchoSpeed gradient system providing a maximum gradient strength of 22 mT/m and maximum slew rate of 120 mT/m/ms (**Figure 1**).

### **1) Structural and microstructural analysis**

## **VBM**

*Data acquisition.* A conventional T1-weighted (T1W) axial volumetric image was acquired using the FSPGR sequence TI=600 ms; TE=5.1 ms; TR=12.5 ms; 25.6 cm square FOV, 1 mm slice thickness; in-plane resolution=256x256.

*Data analysis.* Structural data was analysed with FSL-VBM, a voxel-based morphometry style analysis (Ashburner J and Friston K, 2000) carried out with FSL tools (Smith SM et al, 2004) (**Figure 2**). First, structural images were brain-extracted using BET (Smith SM et al, 2002). Next, tissue-type segmentation was carried out using FAST4 (Zhang Y et al, 2001). The resulting grey-matter partial volume images were then aligned to Montreal Neurological Institute MNI152 standard space using the affine registration tool FLIRT (Jenkinson M et al, 2002], followed by nonlinear registration using FNIRT ([www.fmrib.ox.ac.uk/fsl](http://www.fmrib.ox.ac.uk/fsl)), which uses a b-spline representation of the registration warp field (Rueckert D et al, 1999). The resulting images were averaged to create a study-specific template, to which the native grey matter images were then non-linearly re-registered. The registered partial volume images were then modulated (to correct for local expansion or contraction) by dividing by the Jacobian of the warp field. The modulated segmented images were then smoothed with an isotropic Gaussian kernel with a sigma of 3 mm. Finally, voxelwise GLM was applied using permutation-based non-parametric testing, correcting for multiple comparisons across space, using the program Glm ([www.fmrib.ox.ac.uk/fsl](http://www.fmrib.ox.ac.uk/fsl)), applying threshold-free cluster enhancement. Sex and age were introduced as covariates. Thresholds for significance level were set at  $P < 0.01$ .

## **DTI: ROI/histogram analyses and TBSS**

*Acquisition.* Axial DTI SE-EPI images were obtained (slice thickness = 5 mm, inter-slice gap = 0 mm) using a single-shot EPI sequence with  $\alpha = 90^\circ$ , TE=89.2 ms; TR=10 s; 32 cm<sup>2</sup> FOV, in-plane resolution=192x192,

NEX=1, and phase encoding in right-left direction. Six directions-encoding gradients were applied with gradient strengths corresponding to b-values  $900 \text{ s/mm}^2$ . In addition, images without diffusion weighting were acquired, corresponding to  $b = 0 \text{ s/mm}^2$  and exhibiting T2-contrast.

*Data preprocessing.* Distortions in the DTI-EPI images due to gradient-induced eddy currents were corrected by slice-wise registration of the DT images onto the T2-weighted EPI image using the image registration software FLIRT ([www.fmrib.ox.ac.uk/fsl](http://www.fmrib.ox.ac.uk/fsl)). Due to the nature of the distortions, the degrees of freedom were restricted to translation, scaling, and shearing along the phase encoding direction (Haselgrove et al, 1996). Mean diffusivity (MD) and fractional anisotropy (FA) were determined pixel-wise using a least-squares fit using the program DTIFIT ([www.fmrib.ox.ac.uk/fsl](http://www.fmrib.ox.ac.uk/fsl)). In order to avoid contamination of the MD values for grey and white matter by the much higher values of cerebral spinal fluid (CSF) during further evaluation, pixels containing CSF were masked from the MD map. This was accomplished using the FAST algorithm ([www.fmrib.ox.ac.uk/fsl](http://www.fmrib.ox.ac.uk/fsl)) for a two-class segmentation based on the corresponding T2-weighted EPI images (**Figure 3**).

*Manual ROI and histogram analyses.* Regions of interest (ROIs) were selected manually on T2-weighted EPI images. ROIs were defined to include medulla, pons, left and right middle cerebellar peduncle (MCP), superior cerebellar peduncle (SCP), dentate nucleus, cerebellar white matter, thalamus, caudate, putamen, pallidus, pyramidal tract at the level of the posterior limb of internal capsule (PLIC), frontal and parietal white matter, optic radiation and corpus callosum (genu and splenium) (**Figure 4-A**). Cerebral cortical ROIs were not selected, because substantial partial volume effects from subcortical white matter and CSF could not be completely avoided. For a global evaluation of brain MD values, including cortical areas, histograms of MD were generated for all pixels in the supratentorial and infratentorial compartment (**Figure 4-B/C**). As previously described (Martinelli et al, 2007) infratentorial compartment histograms of MD were also generated separately for areas corresponding

to brainstem, vermis, and cerebellar hemispheres determined by manual segmentation (**Figure 4-D**). The asymmetry of the MD distribution was assessed by finding the 50<sup>th</sup> percentile values (medians) along with the mean (Rizzo et al, 2008) (**Figure 4-E**). Parametric tests were used as Kolmogorov–Smirnov testing showed that means and median values were normally distributed. The Student T test was used to evaluate differences among two groups and Pearson test to evaluate correlations, correcting for multiple comparisons. P values less than 0.05 were accepted as statistically significant.

*Tract-based analysis.* Voxel-wise statistical analysis of the FA data was carried out using TBSS (Tract-Based Spatial Statistics) (Smith SM et al, 2006), part of FSL (Smith SM et al, 2004). First, FA images were created as described in the paragraph 'Data pre-processing'. All subjects' FA data were then aligned into a common space using the nonlinear registration tool FNIRT ([www.fmrib.ox.ac.uk/fsl](http://www.fmrib.ox.ac.uk/fsl)), which uses a b-spline representation of the registration warp field (Rueckert D et al, 1999). Next, the mean FA image was created and thinned to create a mean FA skeleton which represents the centres of all tracts common to the group. Each subject's aligned FA data was then projected onto this skeleton and the resulting data fed into voxelwise cross-subject statistics, correcting for multiple comparisons, using the program Glm ([www.fmrib.ox.ac.uk/fsl](http://www.fmrib.ox.ac.uk/fsl)). Subjects' age and sex were considered nuisance variables whose effect was removed from the final group comparisons. Thresholds for significant level were set at  $P < 0.01$  (**Figure 5**).

#### *Automatic segmentations*

Automatic segmentation of the volumetric T1W image was performed using FIRST ([www.fmrib.ox.ac.uk/fsl](http://www.fmrib.ox.ac.uk/fsl)) to bilaterally define seven subcortical gray matter structures (thalamus, putamen, caudate, pallidus, accumbens, hippocampus and amygdala) (**Figure 6**). In addition, frontal, parietal, temporal and occipital lobes, brainstem and cerebellum were

defined using the MNI152 template. Within these regions gray matter was defined using a three-class segmentation of the T1W images. All structures were registered onto the DTI maps in two steps using FLIRT ([www.fmrib.ox.ac.uk/fsl](http://www.fmrib.ox.ac.uk/fsl)). White matter partial volume on DTI images was masked by registering the MNI FA template onto subjects' own FA map using non-linear registration. Deep gray structures were identified by warping the Harvard-Oxford sub-cortical structure atlas (also defined in MNI coordinate space). A mask excluding CSF was generated from a three-class segmentation of the T2-weighted image volume. ROIs of all deep gray and cortical structures was defined in the DTI space by fusing registered FIRST, Harvard-Oxford, and CSF and WM exclusion masks (**Figure 7**). For each, volumes and median MD values were calculated. Cortical and subcortical volumes were separately corrected for subject age and total brain volume, MD values for age only. Statistical analyses were performed using SPSS 15.0 for Windows. Parametric tests were used as Kolmogorov-Smirnov testing showed that the variables were normally distributed. The Student T test was used to evaluate differences among two groups. For correlations we used the Pearson test. The Bonferroni correction was applied to correct for multiple comparisons. Only P values less than 0.05 were accepted as statistically significant.

## 2) <sup>1</sup>H-MRS

*Data acquisition.* Proton magnetic resonance spectroscopy (<sup>1</sup>H-MRS) study was performed. Single voxel <sup>1</sup>H-MRS spectra were acquired using the PRESS sequence. The water signal was suppressed by the CHESS (Chemical Shift Selective) sequence. A spectrum at short echo-time (TE = 35ms; TR = 4 s; number of acquisitions = 128) was acquired in the medial region of the thalamus (volume 4.0 to 5.0 cm<sup>3</sup>) (**Figure 8**).

*Data analysis.* Peak integrals for N-acetyl-aspartate (NAA), creatine-phosphocreatine (Cr), choline-containing compounds (Cho), and myo-inositol (mI) were calculated using the operator-independent fitting

program LCModel using standard basis sets (Provencher SW, 1993). Peak integral values were expressed relative to Cr. The exclusion criterion for metabolite evaluation was an LCModel estimated fitting error greater than 20%, this being a reliable indicator of poor quality spectra. Statistical analyses were performed using SPSS 15.0 for Windows. Parametric tests were used as Kolmogorov–Smirnov testing showed that the variables were normally distributed. The Student T test was used to evaluate differences among two groups. For correlations we used the Pearson test. For all analyses, only P values less than 0.05 were accepted as statistically significant.

### 3) Phase imaging

*Data acquisition.* Anatomical imaging was performed by a T2-weighted (T2W) FSE sequence in an axial oblique plane, using acquisition parameters:  $\alpha=90^\circ$ ; echo time (TE): 107 ms; repetition time (TR): 5080 ms; square FOV: 24 cm; acquisition matrix 320×256; reconstructed in-plane resolution: 0.938 mm; slice thickness; 4 mm w/o gap. # slices variable to cover whole head. NEX: 2. Phase-sensitized images were acquired using a gradient echo sequence, and preserving both real and imaginary channels. Slice locations matched those of the anatomical scan, excluding slices above the central corpus callosum, and below the dentate nucleus. Acquisition parameters: TE/TR: 40/60 ms; acquisition matrix 512×256; reconstructed in-plane resolution: 0.938 mm; NEX 2; bandwidth 15.6 kHz; maximum acquisition time 7'06".

*Data analysis.* Following the published method (Ogg RJ et al, 1999) data were high pass filtered by multiplication with a filter function in k-space, using tools provided by FSL (FMRIB; U Oxford) and AFNI (NIMH, NIH; Bethesda MD), and a phase map prepared using the filtered data. T2W data were registered onto the gradient echo data using FLIRT (FSL) (**Figure 9**). Whole brain regions of interest were selected automatically

by thresholding T2W data, and excluding pixels whose local filtered phase dispersion exceeded a second threshold (indicating low signal:noise) (**Figure 10**). Regions of interest were selected in two ways: structures known to accumulate iron (dentate and red nucleus, substantia nigra, basal ganglia) were manually segmented using both phase maps and T2W images (**Figure 11**). For whole brain ROIs, the 10<sup>th</sup>, 50<sup>th</sup> and 90<sup>th</sup> percentile of the filtered phase histogram were calculated, while for local ROIs, 25<sup>th</sup> and 50<sup>th</sup> percentiles only, as these contained mainly negative phase. For each percentile score, patients and control groups were compared using the Mann-Whitney U test, and correlation with demographic and clinical parameters used the Spearman test. The Bonferroni correction was applied to correct for multiple comparisons. Statistical analyses will be performed using with SPSS 15.0 for Windows, assuming a significant *P*-value <0.05.

## **RESULTS**

## Structural and microstructural analysis

### *Subjects*

22 patients (age  $50\pm 9$ , mean $\pm$ SD; 7 males and 15 females) and 22 healthy controls (age  $49\pm 16$ , mean  $\pm$  SD; 14 males and 8 females) were studied. Mean values and standard deviations of age at onset, disease duration and IRLSSG score in RLS patients were  $41\pm 12$  years,  $9\pm 8$  years and  $22\pm 7$  respectively. 14 patients never took therapy and 8 patients receiving dopaminergic therapy were free from drugs from at least 2 weeks before scan. 8 patients had a family history of RLS (**Table 2**).

### *MR data*

#### *VBM*

No significant difference in volume or density was found in any brain area. The lack of differences still remains when age and sex were introduced as a cofactor (**Figure 12**).

#### *DTI*

For all ROIs selected MD and FA values in RLS patients were not significantly different from controls (**Table 3**). Similarly, the histograms of MD and FA in the whole sovratentorial and infratentorial compartment and in the brainstem, vermis, and cerebellar hemispheres singly were virtually identical for the two groups and no significant differences were observed at level of median MD values (**Table 3**). TBSS group comparison revealed no difference in MD and FA of any brain area between two groups. The lack of differences still remains when age and sex were introduced as a cofactor (**Figure 13**).

#### *Automatic segmentation*

No significant difference in volume or MD values was disclosed in any segmented structures. (**Table 4**)

## <sup>1</sup>H-MRS

### *Subjects*

25 patients (age 52±10, mean±SD; 10 males and 15 females) and 18 healthy controls (age 51±16, mean ± SD; 11 males and 7 females) were studied. Mean values and standard deviations of age at onset, disease duration and IRLSSG score in RLS patients were 43±13 years, 9±8 years and 22±7 respectively. 16 patients never took therapy and 9 patients receiving dopaminergic therapy were free from drugs from at least 2 weeks before scan. 9 patients had a family history of RLS (**Table 5**).

### *MR data*

The NAA/Cr and Cho/Cr ratios were significantly lower in the medial thalamus of RLS patients compared with the healthy controls (**Table 6, Figures 14 and 15**). We did not detect statistical differences in the other ratios. The reduction of the NAA/Cr and Cho/Cr ratios in the thalamus of the patients did not correlate with the clinical variables considered (age, age at onset, disease duration, IRLSSG rating scale for symptoms severity).

## Phase imaging

### *Subjects*

11 patients (age 54±11, mean±SD; 2 males and 9 females) and 11 healthy controls (age 51±18, mean ± SD; 6 males and 5 females) were studied. Mean values and standard deviations of age at onset, disease duration and IRLSSG score in RLS patients were 48±11 years, 6±3 years and 21±9

respectively. 8 patients never took therapy and 3 patients receiving dopaminergic therapy were free from drugs from at least 2 weeks before scan. 5 patients had a family history of RLS (**Table 7**).

### ***MR data***

In the whole brain analysis, RLS patients showed lower phase dispersion, characterized by 10<sup>th</sup> and 90<sup>th</sup> percentile radians values of significantly smaller magnitude than in controls (respectively  $p=0.01$  and  $p=0.02$ ), while the median was no different (**Table 8 and Figure 16**). In the localized ROIs, differences were not significant although there was a trend of more negative radians values, prevalently in red nucleus and substantia nigra (**Table 8**). The 10<sup>th</sup> percentile of whole brain phase in RLS patients correlated with disease duration ( $r=0.60$ ,  $p=0.04$ ) (**Figure 17**), but not with IRLSSG rating scale or other clinical/demographic parameters.

## **DISCUSSION**

In this study we have used advanced MR techniques to investigate various aspects of RLS pathophysiology. Firstly, we used a multimodal approach to evaluate the possible presence of structural and/or microstructural abnormalities in terms of volume and/or DTI parameters alterations using ROI/histogram analysis, VBM, TBSS and automatic segmentations of brain structures. Neither volume or MD or FA pathological changes were found in any brain structures of RLS patients. Regarding four previous VBM studies (Etgen T et al, 2005; Unrath A et al, 2007; Hornyak M et al, 2007; Celle S et al, 2009) our data are in accord only with the most recent one which found a lack of specific grey matter alterations in RLS patients (Celle S et al, 2009). Discrepancies with other studies might on the one hand be explained by methodological differences, since the first study, detecting increasing pulvinar grey matter, was performed by use of the classical VBM technique (Etgen T et al, 2005). All other studies, including our, used the optimised VBM protocol (Good CD et al, 2001). Differently from previous studies, our study used the software FSL-VBM instead of SPM, although the two software packages seem to give similar results (Battaglini M et al, 2009). For example Cell et al found results very similar to ours, using SPM. Another important note regarding the first two VBM works is that in neither study did the results survive a correction for multiple comparisons (Etgen T et al, 2005; Unrath A et al, 2007).

Methodological differences are also present between our and a previous DTI analysis (Unrath A et al, 2008), which disclosed an FA reduction in the sensori-motor cortical regions not confirmed in our study. Indeed, Unrath et al used standard registration algorithms that didn't give a satisfactory solution to the question of how to align FA images from multiple subjects with an arbitrariness of the choice of spatial smoothing extent. We have chosen to use TBSS, which resolves these issues by using the "mean FA skeleton" approach (Smith SM et al, 2006 and 2007). Lack of any MD or FA abnormalities was confirmed by the ROI and histogram analysis. Furthermore for the first time in RLS patients we evaluated volume and DTI

parameters at level of cortical and subcortical areas using automatic segmentation and again no pathological changes were present.

On the other hand, these technical aspects alone might not be sufficient to explain the different results among different studies. The heterogeneity in terms of size and clinical features of the studied samples could be a considerable factor. The presence of medical treatment, such as dopaminergic agents, is an important issue, because these are known to affect the morphology of cerebral structures (Corson PW et al, 1999). In some studies (Etgen T et al, 2005; Unrath A et al, 2007 and 2008) almost all the patients were on treatment, but not in all cases (Hornyak M et al, 2007; Celle S et al, 2009). In our sample most patients (n=16) never took therapy. In the remaining 9 patients treated with dopaminergic drugs, treatment was stopped for at least 2 weeks before scan. Other possible differences among the studies would regard the severity of symptoms, the percentage of family history, and the co-occurrence of other sleep disorders. Finally the possible heterogeneity of RLS itself might be reflected in the different results.

Overall our VBM and DTI data argue against clear structural/microstructural abnormalities in the brain of patients with idiopathic RLS.

The second part of our study focused on thalamic involvement. Using <sup>1</sup>H-MRS we detected metabolic changes in the medial region of the thalamus. This region is a part of the medial nociceptive system. This system projects through medial and intralaminar nuclei of the thalamus to several cortical and limbic regions: frontal and insular cortices and anterior cingulate gyrus. It is thought to mediate affective-motivational aspects of pain such as emotional reactions, arousal and attention to the stimulus, as well as the drive to escape from the noxious stimuli (Treede RD et al, 1999; Price DD, 2000). An activation of these brain structures during pain perception has been confirmed by PET and fMRI studies (Apkarian AV et al, 2005). H<sub>2</sub>[<sup>15</sup>O] PET (San Pedro EC et al, 1998) and fMRI (Bucher SF et al, 1997; Astrakas LG et al, 2008) found similar brain activation in RLS patients. A PET study with [<sup>11</sup>C]diprenorphine, a non-selective opioid receptor

radioligand, disclosed regional negative correlations between ligand binding and RLS severity in areas serving the medial pain system (medial thalamus, amygdala, caudate nucleus, anterior cingulate gyrus, insular cortex and orbitofrontal cortex) (von Spiczak S et al, 2005). Another PET study which used the high-affinity D2-receptors radioligands [<sup>11</sup>C]FLB 457 reported a higher thalamic binding potential in RLS patients than in controls, at the level of the medial and posterior portions, other than at the level of limbic and associative part of striatum, anterior cingulate cortex and insulae, suggesting again an involvement of the medial pain system (Cervenka S et al, 2006). Neurophysiological studies have shown an impairment of pain and temperature perception in idiopathic RLS, with an absence of peripheral nerve fibre damage suggesting a functional impairment of central somatosensory processing (Stiasny-Kolster K et al, 2004; Schattschneider J et al, 2004; Tyvaert L et al, 2009b). Interestingly one study has disclosed increased ratings of pin-prick pain in untreated RLS patients indicating static hyperalgesia that was more pronounced in the lower limb and reversed by long-term dopaminergic treatment (Stiasny-Kolster K et al, 2004).

Our MR spectroscopic data confirm a thalamic involvement in RLS patients, presumably not due to degenerative changes given that none were detected by VBM and DTI studies (see above). This abnormality could be an epiphenomenon in the pathophysiology of RLS, in terms of metabolic dysfunction secondary to discomfort perception. But it is also possible that the involvement of the medial portion of the thalamus could have a primary role, because its function is modulated by dopaminergic afferents. Indeed, an extensive mesothalamic and nigrothalamic system originates as collaterals from A8-A9-A10 neurons (Freeman A et al, 2001). Thus, DA axons directly innervate thalamic components of several parallel, functionally unique, basal ganglia-thalamocortical loops as follows: motor (ventrolateral; VL), ‘prefrontal’ (parvocellular ventroanterior; VApc), and ‘limbic’ (mediodorsal; MD) in non-human primates and humans (Rye DB, 2004).

From this point of view the thalamic metabolic alteration which we have found may reflect an impairment of medial pain system secondary to a dopaminergic dysfunction and leading to a abnormal affective-motivational sensory-motor processing of the sensory inputs. This could also happen in parallel with a dysfunction of other dopaminergic pathways such as the diencephalospinal pathway projecting from A11 area to spinal cord in a contest of a multilevel demodulation of pain stimuli perception.

The third part of our study investigated the brain iron content of RLS patients and disclosed a global brain iron reduction in these patients compared to healthy subjects of a similar age. We used a quantitative evaluation of the phase maps obtained by a SWI protocol. Paramagnetic tissue causes a dipolar effect and iron presence strictly affects the paramagnetic properties of the tissues (Ogg RJ et al, 1999). In our work alterations were seen in both the 10th and the 90th percentile of the whole brain histogram where the extremes of image phase variation were reduced, due to reduced paramagnetic tissue content in RLS subjects. This is consistent with a lower iron content compared to normal brains. This alteration correlated with disease duration. These data are in agreement with the previous MRI studies that found increased T2, T2\* and T2' (and reduced R2, R2\* and R2') in different brain structures including substantia nigra, thalamus and caudate (Allen RP et al, 2001; Earley CJ et al, 2006; Astrakas LG et al, 2008; Godau J et al, 2008). Variability in these results points toward a non localized reduced iron content but most probably a diffuse lowering. Indeed despite the small sample size we found an alteration at the whole brain analysis, which appears to be more sensitive than the local ROI analysis where we did not detect significant differences but only a trend. Alterations of iron regulatory proteins such as ferritin, divalent metal transporter 1, ferroportin, transferrin, transferrin receptor, pro-hepcidin and hepcidin detected in neuromelanin cells and CSF from brains of patients (Clardy SL et al, 2006b; Connor JR et al, 2003 and 2004) indicate a basic alteration of brain iron homeostasis, probably affecting the control of iron movement between CSF and brain and between extracellular and

intracellular compartments. Iron deficiency should impair the function of some cerebral systems more than others, notably the dopaminergic system, because of the strong connection between dopamine and iron (Allen RP, 2004; Allen RP and Earley CJ, 2007). Under this hypothesis, an involvement of all the various dopaminergic pathways could be present at a subclinical level, but only that of networks implicated in sensori-motor integration and pain processing would be clearly evident at clinical level, either because of a further major susceptibility to iron deficiency in neurons in this network, or because of differences in the threshold of perceptibility of the dysfunction (sensory dysfunction through pain system rather than motor impairment through nigrostriatal system for example).

A methodological consideration coming from our study is that the histogram analysis of the phase maps is a very sensitive tool to evaluate brain iron content and is also far less operator dependent. This suggests that this imaging protocol may also be useful in all types of neurological disease characterized by a pathological increase of iron accumulation, primary (neurodegeneration with brain iron accumulation) or secondary (neurodegenerative diseases), as a biomarker of disease progression and for assessment of pharmacological interventions with chelating drugs.

In summary, putting together the results of all the different MR protocols adopted in this study, we can support a pathophysiological model of RLS which is consistent with low brain iron content in the brains of these patients. The iron deficiency may lead to a functional impairment, in the absence of structural and/or microstructural abnormalities. Via dopaminergic dysfunction, this functional impairment affects the central mechanisms of sensori-motor integration and pain processing involving a number of brain structures including the medial thalamus (part of medial pain system).

## **TABLES AND FIGURES**

**Table 1.** Patients recruited for MR studies. All patients performed the <sup>1</sup>H-MRS study. \*=performed structural-microstructural study. #=performed phase imaging study.

| <b>Patients</b> | <b>Age (y)</b> | <b>Sex</b> | <b>Age at onset (y)</b> | <b>Disease length (y)</b> | <b>Therapy</b> | <b>Family history</b> | <b>IRLSSGRS score</b> |
|-----------------|----------------|------------|-------------------------|---------------------------|----------------|-----------------------|-----------------------|
| 1*              | 48             | M          | 45                      | 3                         | /              | No                    | 22                    |
| 2*              | 49             | F          | 39                      | 10                        | /              | No                    | 21                    |
| 3*              | 46             | M          | 15                      | 31                        | DA drugs       | Yes                   | 26                    |
| 4*              | 43             | F          | 40                      | 3                         | /              | No                    | 24                    |
| 5*              | 43             | F          | 35                      | 8                         | /              | No                    | 26                    |
| 6*              | 55             | F          | 48                      | 7                         | /              | No                    | 23                    |
| 7*              | 43             | F          | 19                      | 24                        | DA drugs       | No                    | 25                    |
| 8*              | 56             | M          | 40                      | 16                        | DA drugs       | Yes                   | 21                    |
| 9*              | 31             | M          | 30                      | 1                         | /              | Yes                   | 22                    |
| 10*             | 50             | F          | 24                      | 26                        | DA drugs       | No                    | 26                    |
| 11              | 66             | M          | 59                      | 7                         | DA drugs       | Yes                   | 28                    |
| 12*             | 50             | M          | 49                      | 1                         | /              | No                    | 8                     |
| 13*             | 58             | M          | 56                      | 2                         | DA drugs       | No                    | 24                    |
| 14*             | 67             | M          | 57                      | 10                        | /              | No                    | 20                    |
| 15*#            | 65             | F          | 58                      | 7                         | /              | Yes                   | 24                    |
| 16*#            | 50             | F          | 40                      | 10                        | DA drugs       | No                    | 24                    |
| 17#             | 58             | M          | 54                      | 4                         | /              | No                    | 22                    |
| 18#             | 69             | F          | 66                      | 3                         | /              | No                    | 10                    |
| 19*#            | 56             | M          | 51                      | 5                         | DA drugs       | No                    | 30                    |
| 20*#            | 48             | F          | 38                      | 10                        | /              | No                    | 28                    |
| 21*#            | 49             | F          | 45                      | 4                         | /              | Yes                   | 9                     |
| 22*#            | 45             | F          | 40                      | 5                         | /              | No                    | 12                    |
| 23*#            | 31             | F          | 25                      | 6                         | /              | Yes                   | 11                    |
| 24*#            | 62             | F          | 50                      | 12                        | DA drugs       | Yes                   | 35                    |
| 25*#            | 61             | F          | 57                      | 4                         | /              | Yes                   | 21                    |
| <b>Mean</b>     | <b>52</b>      |            | <b>43</b>               | <b>9</b>                  | <b>9/16</b>    | <b>9/16</b>           | <b>22</b>             |
| <b>SD</b>       | <b>10</b>      |            | <b>13</b>               | <b>8</b>                  | <b>/</b>       | <b>/</b>              | <b>7</b>              |

DA drugs = dopaminergic drugs; IRLSSGRS = International Restless Legs Syndrome Study Group Rating Scale

**Figure 1.** 1.5 Tesla GE Signa Horizon LX system equipped with a birdcage head radio-frequency coil for signal reception.



**Figure 2.** Schematic illustration of methodological steps of FSL-VBM (from [www.fmrib.ox.ac.uk/fsl](http://www.fmrib.ox.ac.uk/fsl)). A: Original T1-weighted volumetric images; B: Segmented grey matter partial volume; C: spatially smoothed grey matter partial volume; D: Regions of significant group difference in GM volume (colour) superimposed on template T1-weighted image.

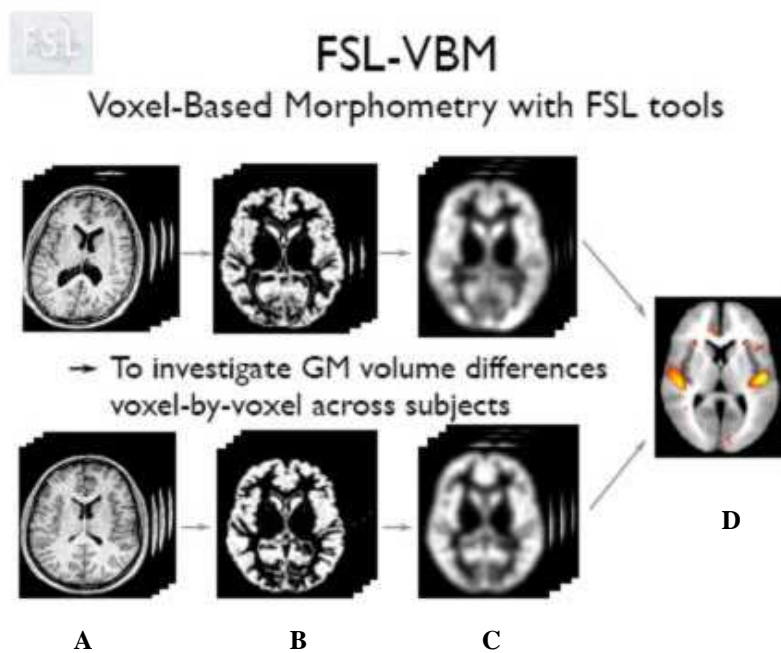


**Figure 3.** Schematic illustration of preprocessing of DTI images for FA/MD analysis. A: DTI image. B: T2W image. C: MD map. D: First eigenvector map weighted by FA.

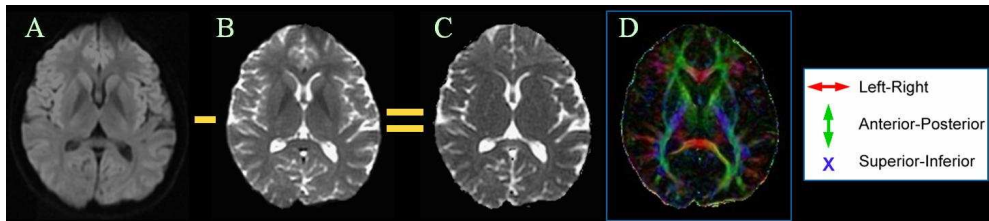


**Figure 4.** A: Example of manual segmentation of ROIs. B-D: manual segmentation of whole left and right hemispheres (B), whole infratentorial compartment (C) and of the areas corresponding to brainstem, vermis, and cerebellar hemispheres separately for histogram analysis (D). E: example of cerebral hemisphere histograms in a healthy control.

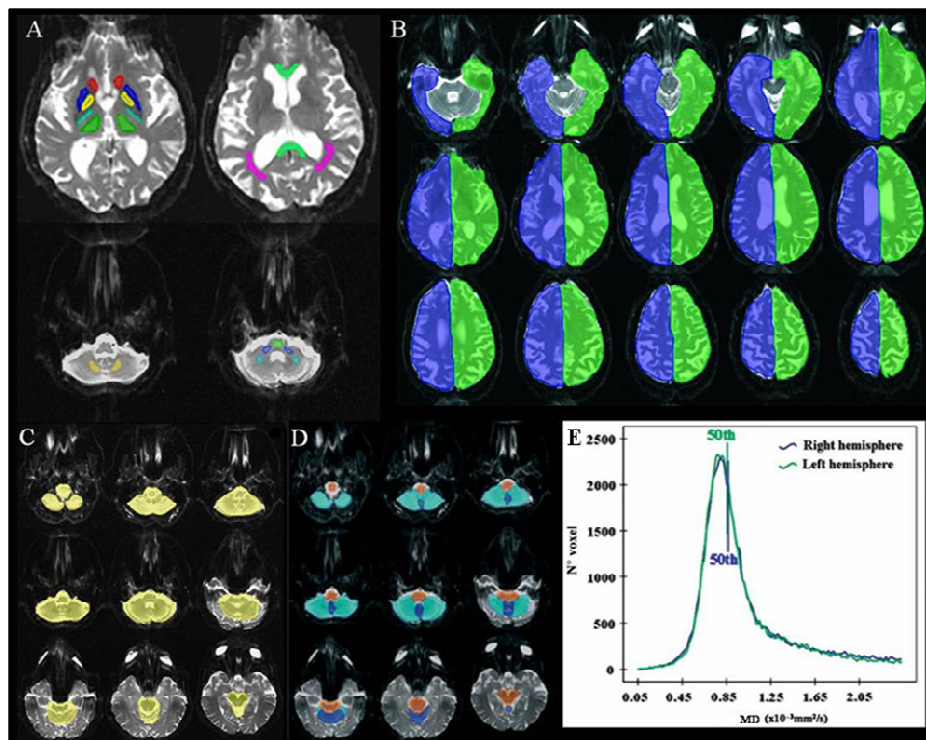


**Figure 5.** Schematic illustration of methodological steps of TBSS (from [www.fmrib.ox.ac.uk/fsl](http://www.fmrib.ox.ac.uk/fsl)).

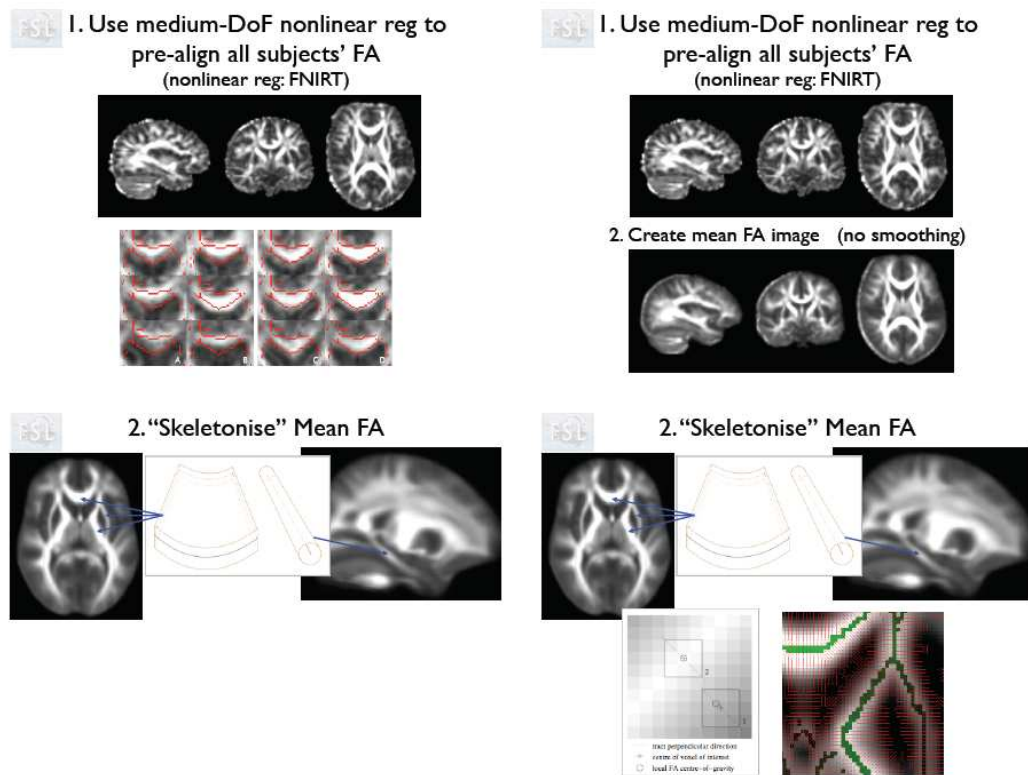


**Figure 6.** Example of three dimensional projection of automatically generated subcortical structures (colour) onto T1-weighted volumetric image (greyscale).

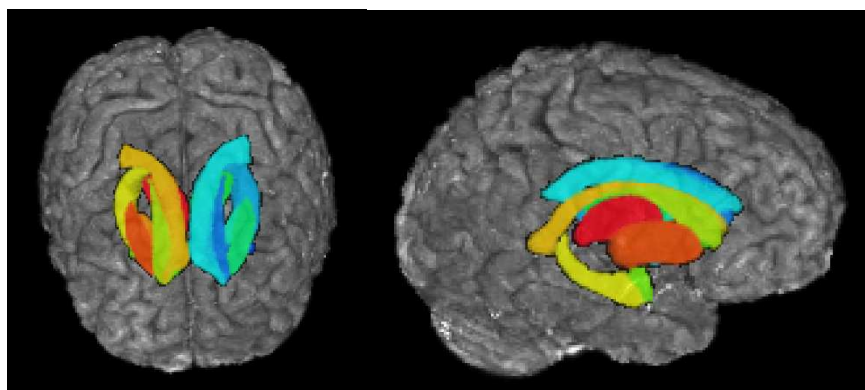


**Figure 7.** Data pipeline to create automatic ROIs.

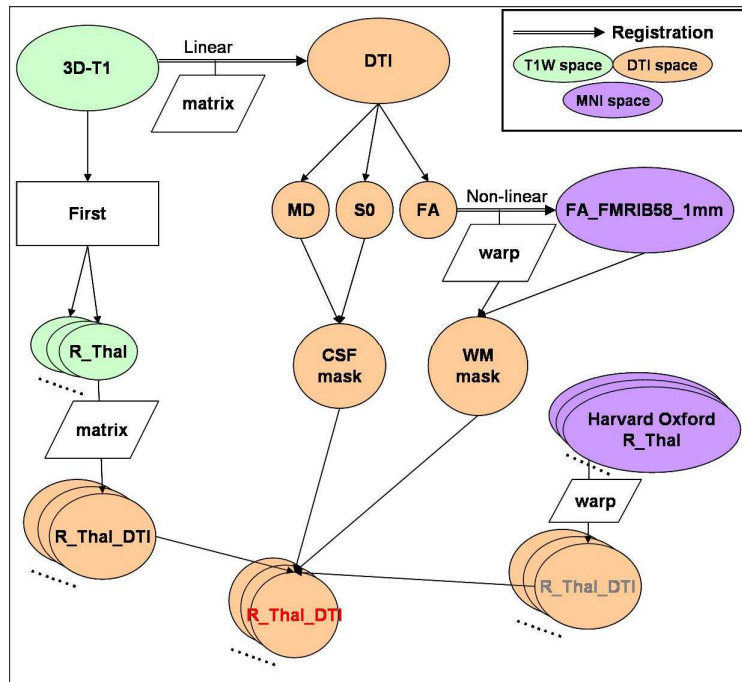


**Figure 8.** Localization of medial thalamic VOI (volume of interest) for  $^1\text{H}$ -MRS study (A) and example of spectrum (B) in a control subject. NAA = N-acetyl-aspartate; Cr = creatine-phosphocreatine; Cho = choline-containing compounds; mI = myo-inositol.

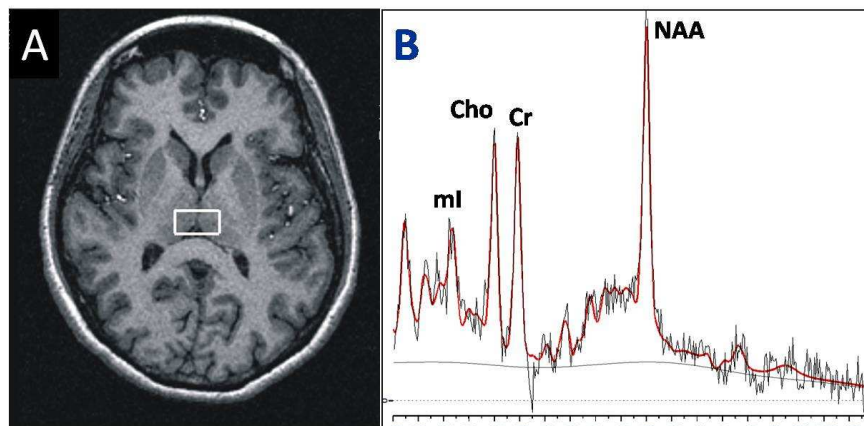


**Figure 9.** Schematic illustration of preprocessing of phase images. A-B: real and imaginary images; C-D: Low pass filtered images; E: phase map; F-H: details of iron-rich structures (F: basal ganglia, G: substantia nigra and red necluei, H: dentate nuclei).

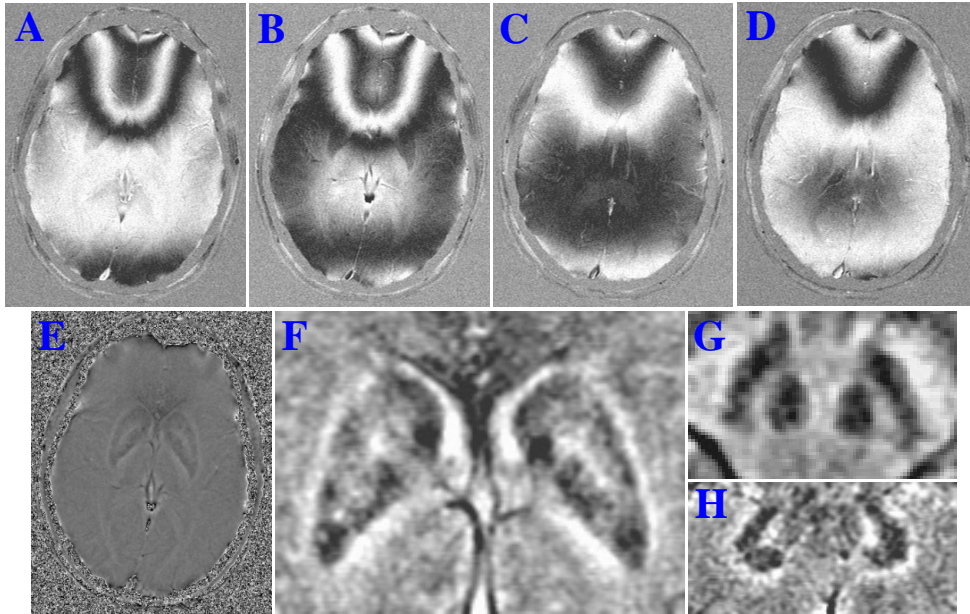


**Figure 10.** Whole brain ROI (A) and derived phase histogram from a healthy control (B).

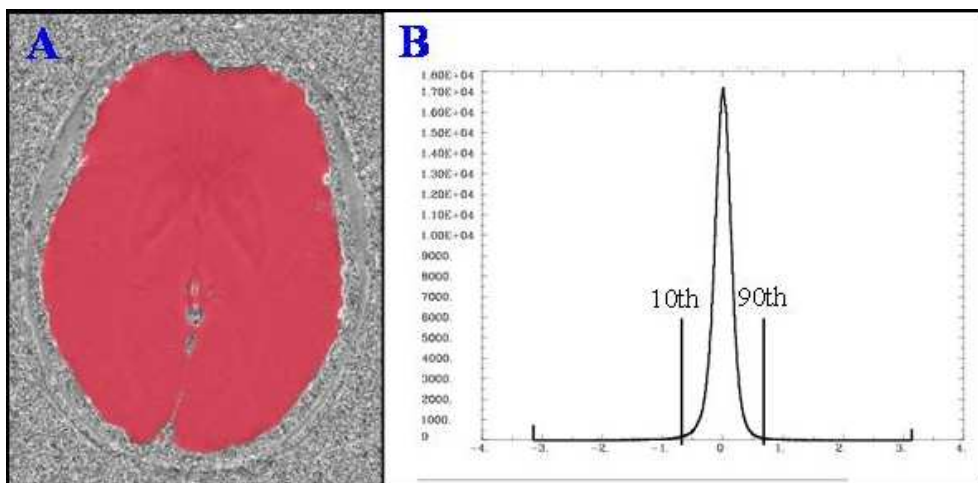


**Figure 11.** Manual segmentation of ROIs at level of iron-rich structures (A: basal ganglia, B: substantia nigra and red nucleus, C: dentate nuclei).

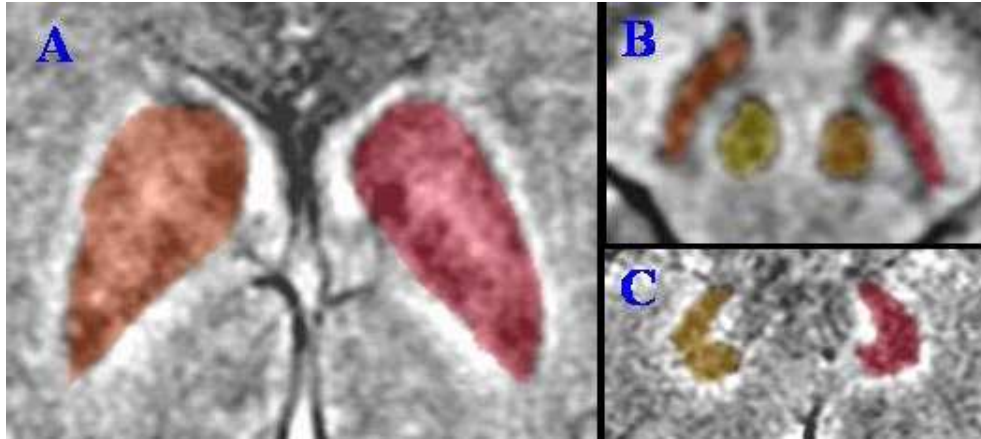


**Table 2.** Clinical data of the RLS patients and controls of the structural/microstructural study.

| Subjects (N)          | Age (years) | Sex (M/F) | Age at onset (years) | Disease duration (years) | IRLSSG score | Therapy (DA drugs) (N) | Positive family history (N) |
|-----------------------|-------------|-----------|----------------------|--------------------------|--------------|------------------------|-----------------------------|
| RLS patients (22)     | 50±9        | 7/15      | 41±12                | 9±8                      | 22±7         | 8 (36%)                | 8 (36%)                     |
| Healthy controls (22) | 49±16       | 14/8      | /                    | /                        | /            | /                      | /                           |

M, male; F, female; DA drugs = Dopaminergic drugs; IRLSSGRS = International Restless Legs Syndrome Study Group Rating Scale. All data are given as mean ± SD.

**Figure 12.** VBM analysis disclosed no differences between two groups. Thresholds for significance level were set at  $P < 0.01$  after correction for multiple comparisons across space, and applying threshold-free cluster enhancement.

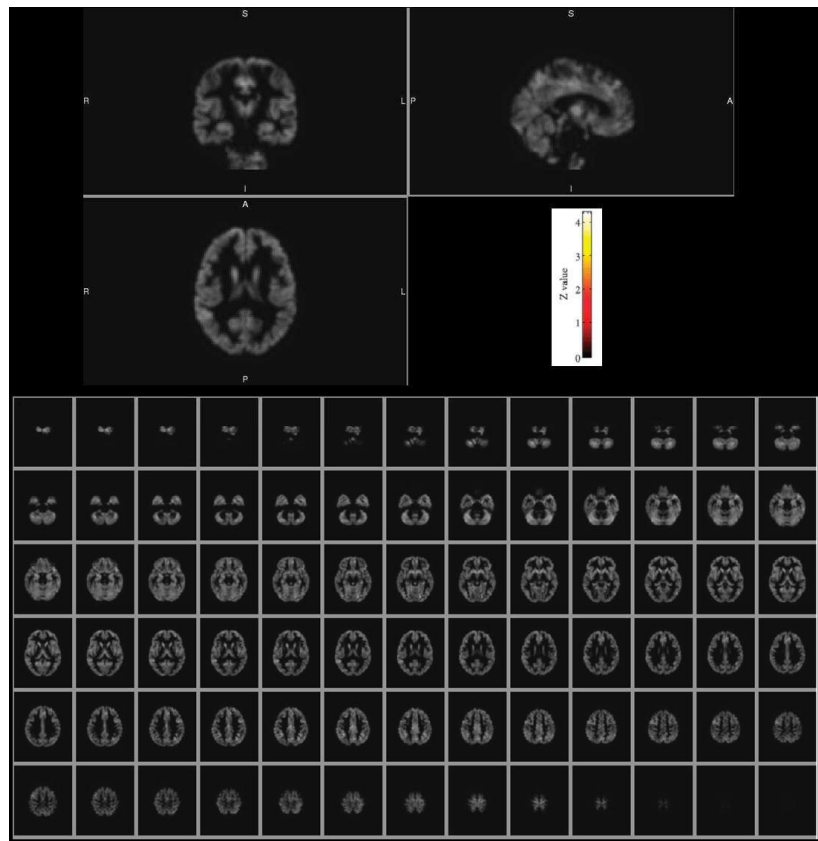


**Table 3.** MD and FA values for control and RLS groups by ROI and histogram analysis of DTI images.

| ROIs  | MD ( $\times 10^{-3}$ mm <sup>2</sup> /s) |              | FA        |              | P*   |
|---|---|--------------|-----------|--------------|------|
|   | Controls                                  | RLS patients | Controls  | RLS patients |      |
| <b>Mean values</b>                              |   |              |           |              |      |
| Medulla   | 0.84±0.07                                 | 0.86±0.08    | 0.46±0.12 | 0.44±0.10    | n.s. |
| Dentate nucleus <sup>#</sup>                    | 0.69±0.06                                 | 0.74±0.06    | 0.34±0.07 | 0.31±0.07    | n.s. |
| Pons  | 0.87±0.06                                 | 0.91±0.05    | 0.43±0.07 | 0.47±0.08    | n.s. |
| Middle cerebellar peduncle <sup>#</sup>         | 0.74±0.06                                 | 0.78±0.05    | 0.60±0.04 | 0.57±0.07    | n.s. |
| Superior cerebellar peduncle <sup>#</sup>       | 0.69±0.03                                 | 0.69±0.05    | 0.48±0.10 | 0.43±0.10    | n.s. |
| Cerebellar white matter <sup>#</sup>            | 0.81±0.04                                 | 0.77±0.06    | 0.67±0.07 | 0.69±0.06    | n.s. |
| Posterior limb of internal capsule <sup>#</sup> | 0.69±0.03                                 | 0.71±0.03    | 0.68±0.04 | 0.52±0.07    | n.s. |
| Thalamus <sup>#</sup>                           | 0.78±0.02                                 | 0.78±0.05    | 0.32±0.02 | 0.70±0.04    | n.s. |
| Putamen <sup>#</sup>                            | 0.75±0.02                                 | 0.75±0.02    | 0.24±0.03 | 0.33±0.03    | n.s. |
| Globus pallidus <sup>#</sup>                    | 0.73±0.03                                 | 0.75±0.04    | 0.38±0.04 | 0.23±0.03    | n.s. |
| Caudate <sup>#</sup>                            | 0.79±0.03                                 | 0.80±0.03    | 0.24±0.03 | 0.38±0.04    | n.s. |
| Parietal white matter <sup>#</sup>              | 0.85±0.07                                 | 0.84±0.06    | 0.39±0.07 | 0.22±0.02    | n.s. |
| Frontal white matter <sup>#</sup>               | 0.78±0.04                                 | 0.76±0.03    | 0.29±0.04 | 0.41±0.05    | n.s. |
| Corpus callosum <sup>###</sup>                  | 0.82±0.05                                 | 0.83±0.04    | 0.76±0.03 | 0.29±0.04    | n.s. |
| Optic radiation <sup>#</sup>                    | 0.83±0.04                                 | 0.83±0.03    | 0.55±0.04 | 0.76±0.05    | n.s. |
| <b>Median values</b>                            |   |              |           |              |      |
| Sovratentorial compartment                      | 0.89±0.05                                 | 0.86±0.03    | 0.23±0.02 | 0.24±0.02    | n.s. |
| Infratentorial compartment                      | 0.87±0.05                                 | 0.87±0.05    | 0.29±0.04 | 0.31±0.04    | n.s. |
| Brainstem                                       | 0.90±0.05                                 | 0.87±0.05    | 0.44±0.04 | 0.45±0.02    | n.s. |
| Vermis  | 0.98±0.11                                 | 0.96±0.07    | 0.23±0.03 | 0.24±0.04    | n.s. |
| Cerebellar hemispheres                          | 0.81±0.03                                 | 0.83±0.05    | 0.29±0.05 | 0.30±0.05    | n.s. |

\*Student T test (a *P*-value of <0.05 after correction for multiple comparisons was considered to be significant). MD= Mean diffusivity; FA= Fractional anisotropy. <sup>#</sup> = Mean of the left and right values. <sup>###</sup> = Mean of the genu and splenium. All data are given as mean ± SD.

**Figure 13.** TBSS analysis of DTI images disclosed no differences between two groups. Thresholds for significance level were set at  $P < 0.01$  after correction for multiple comparisons across space, and applying threshold-free cluster enhancement.

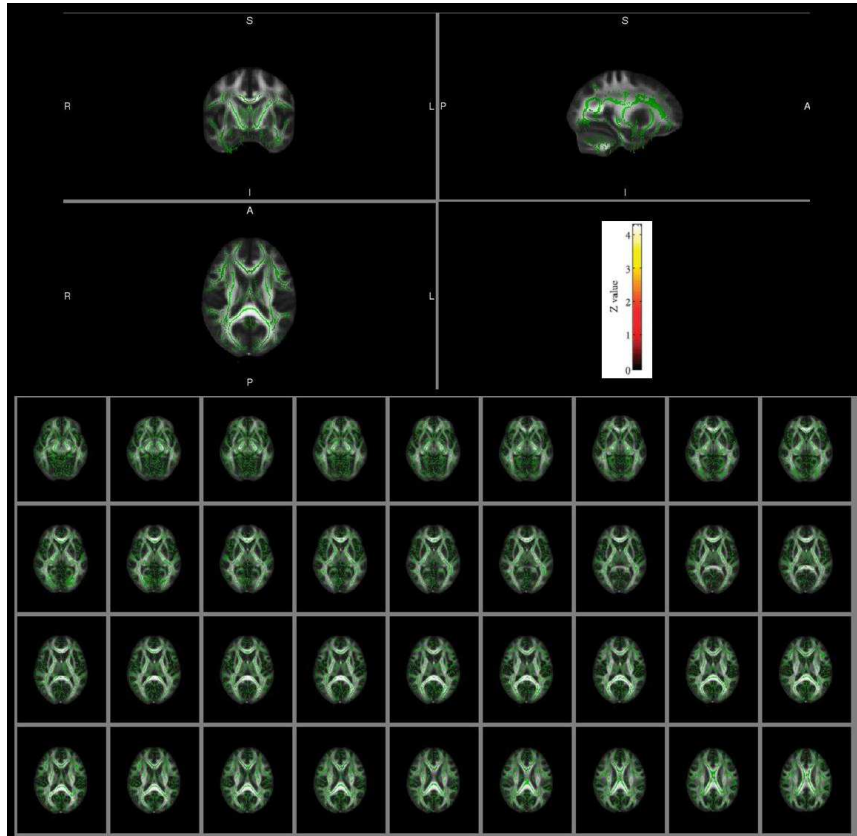


**Table 4.** MD values and volumes for control and RLS groups selected by automatic ROI segmentation.

| <b>Volume (mm<sup>3</sup>)</b>                |                 |            |                     |            |           |
|---|-----------------|------------|---------------------|------------|-----------|
|   | <b>Controls</b> |            | <b>RLS patients</b> |            | <b>P*</b> |
|   | <b>Mean</b>     | <b>±SD</b> | <b>Mean</b>         | <b>±SD</b> |           |
| Occipital lobe <sup>#</sup>                   | 101259          | 12651      | 98645               | 9738       | n.s.      |
| Parietal lobe <sup>#</sup>                    | 149318          | 15213      | 148619              | 14795      | n.s.      |
| Temporal lobe <sup>#</sup>                    | 141164          | 11859      | 140741              | 15285      | n.s.      |
| Frontal lobe <sup>#</sup>                     | 239190          | 26608      | 239435              | 23835      | n.s.      |
| Caudate <sup>#</sup>                          | 7199            | 708        | 6712                | 819        | n.s.      |
| Pallidus <sup>#</sup>                         | 3572            | 447        | 3450                | 391        | n.s.      |
| Putamen <sup>#</sup>                          | 9680            | 1315       | 9441                | 926        | n.s.      |
| Thalamus <sup>#</sup>                         | 15572           | 1829       | 14862               | 1333       | n.s.      |
| Accumbens <sup>#</sup>                        | 1033            | 185        | 1101                | 156        | n.s.      |
| Hippocampus <sup>#</sup>                      | 7822            | 1077       | 7633                | 518        | n.s.      |
| Amygdala <sup>#</sup>                         | 2775            | 389        | 2630                | 474        | n.s.      |
| Brainstem                                     | 23566           | 2804       | 21650               | 9455       | n.s.      |
| Cerebellum                                    | 110160          | 11203      | 104524              | 10450      | n.s.      |
| <b>MD (x10<sup>-3</sup> mm<sup>2</sup>/s)</b> |                 |            |                     |            |           |
|   | <b>Controls</b> |            | <b>RLS patients</b> |            | <b>P*</b> |
|   | <b>Mean</b>     | <b>±SD</b> | <b>Mean</b>         | <b>±SD</b> |           |
| Occipital lobe <sup>#</sup>                   | 0,84            | 0,04       | 0,81                | 0,03       | n.s.      |
| Parietal lobe <sup>#</sup>                    | 0,79            | 0,04       | 0,77                | 0,03       | n.s.      |
| Temporal lobe <sup>#</sup>                    | 0,85            | 0,03       | 0,83                | 0,02       | n.s.      |
| Frontal lobe <sup>#</sup>                     | 0,80            | 0,04       | 0,79                | 0,02       | n.s.      |
| Caudate <sup>#</sup>                          | 0,77            | 0,02       | 0,80                | 0,02       | n.s.      |
| Pallidus <sup>#</sup>                         | 0,77            | 0,06       | 0,76                | 0,02       | n.s.      |
| Putamen <sup>#</sup>                          | 0,75            | 0,02       | 0,74                | 0,02       | n.s.      |
| Thalamus <sup>#</sup>                         | 0,79            | 0,05       | 0,78                | 0,04       | n.s.      |
| Accumbens <sup>#</sup>                        | 0,80            | 0,05       | 0,80                | 0,03       | n.s.      |
| Hippocampus <sup>#</sup>                      | 0,92            | 0,04       | 0,91                | 0,04       | n.s.      |
| Amygdala <sup>#</sup>                         | 0,86            | 0,05       | 0,87                | 0,04       | n.s.      |
| Brainstem                                     | 0,83            | 0,03       | 0,85                | 0,05       | n.s.      |
| Cerebellum                                    | 0,79            | 0,03       | 0,80                | 0,04       | n.s.      |

\*Student T test (a *P*-value of <0.05 after correction for multiple comparisons was considered to be significant). MD= mean diffusivity. <sup>#</sup> = Mean of the left and right values.

**Table 5.** Clinical data of the RLS patients and controls of the <sup>1</sup>H-MRS study.

| Subjects<br>(N)             | Age<br>(years) | Sex<br>(M/F) | Age at<br>onset<br>(years) | Disease<br>duration<br>(years) | IRLSSG<br>score | Therapy<br>(DA<br>drugs)<br>(N) | Positive<br>family<br>history<br>(N) |
|-----------------------------|----------------|--------------|----------------------------|--------------------------------|-----------------|---------------------------------|--------------------------------------|
| RLS<br>patients<br>(25)     | 52±10          | 10/15        | 43±13                      | 9±8                            | 22±7            | 9 (36%)                         | 9 (36%)                              |
| Healthy<br>controls<br>(18) | 51±16          | 11/7         | /                          | /                              | /               | /                               | /                                    |

M, male; F, female; DA drugs = dopaminergic drugs; IRLSSGRS = International Restless Legs Syndrome Study Group Rating Scale. All data are given as mean ± SD.

**Table 6.** <sup>1</sup>H-MRS results in RLS patients and healthy controls.

|        | Ratios   |      |              |      | <i>P</i> * |
|--------|----------|------|--------------|------|------------|
|        | Controls |      | RLS patients |      |            |
|        | Mean     | ±SD  | Mean         | ±SD  |            |
| NAA/Cr | 1.39     | 0.11 | 1.24         | 0.16 | <0.01      |
| Cho/Cr | 0.31     | 0.04 | 0.29         | 0.03 | <0.05      |
| mI/Cr  | 0.83     | 0.17 | 0.78         | 0.13 | n.s.       |

\*Student T test (a *P*-value of <0.05 was considered to be significant). NAA = N-acetyl-aspartate; Cr = creatine-phosphocreatine; Cho = choline-containing compounds; mI = myo-inositol.

**Figure 14.** Examples of medial thalami spectra in one RLS patient and one control. NAA = N-acetyl-aspartate; Cr = creatine-phosphocreatine; Cho = choline-containing compounds; mI = myo-inositol.

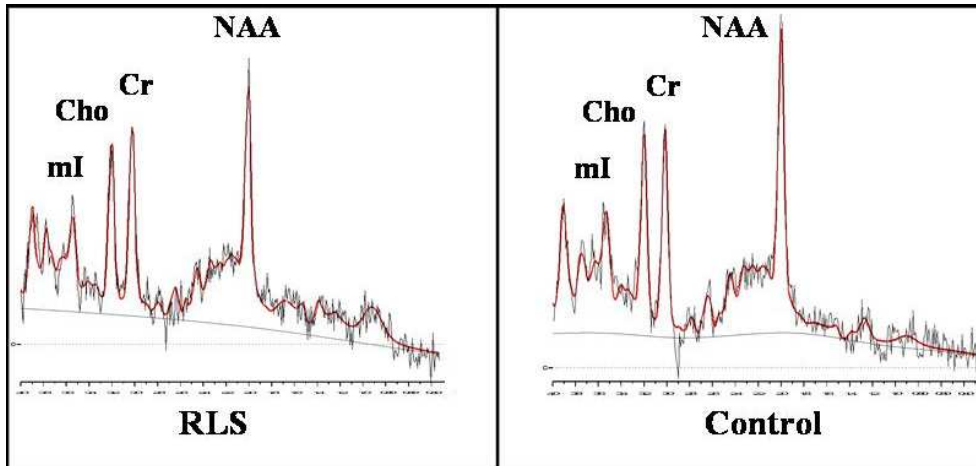
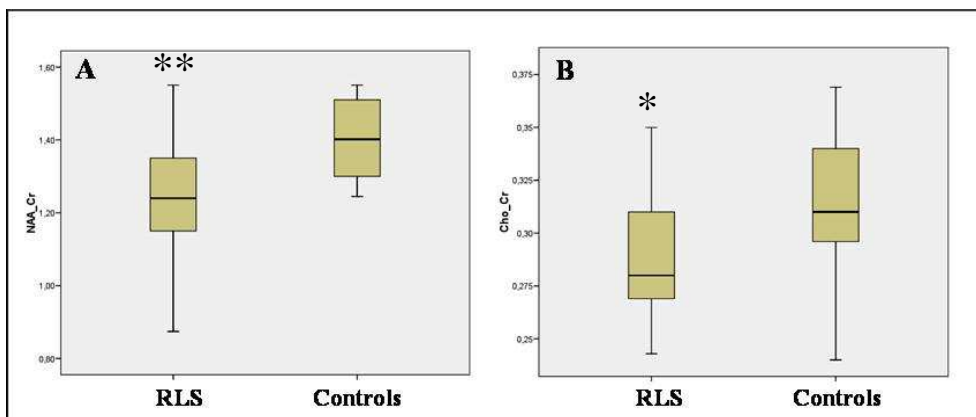


**Figure 15.** Box-plots of <sup>1</sup>H-MRS data of RLS patients and controls (A: NAA/Cr; B: Cho/Cr).



\*\*=P<0.01; \*=P<0.05

**Table 7.** Clinical data of the RLS patients and controls of the phase imaging study.

| Subjects<br>(N)  | Age<br>(years) | Sex<br>(M/F) | Age at<br>onset<br>(years) | Disease<br>duration<br>(years) | IRLSSG<br>score | Therapy<br>(DA<br>drugs)<br>(N) | Positive<br>family<br>history<br>(N) |
|------------------|----------------|--------------|----------------------------|--------------------------------|-----------------|---------------------------------|--------------------------------------|
| RLS              |                |              |                            |                                |                 |                                 |                                      |
| patients<br>(11) | 54±11          | 2/9          | 48±11                      | 6±3                            | 21±9            | 3 (27%)                         | 5 (46%)                              |
| Healthy          |                |              |                            |                                |                 |                                 |                                      |
| controls<br>(11) | 51±18          | 6/5          | /                          | /                              | /               | /                               | /                                    |

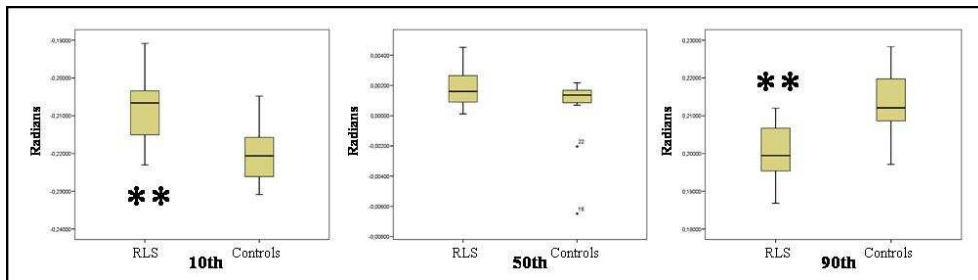
M, male; F, female; DA drugs = dopaminergic drugs; IRLSSGRS = International Restless Legs Syndrome Study Group Rating Scale. All data are given as mean ± SD.

**Table 8.** Phase image analysis of RLS patients and controls.

|                                    | Phase (radians) |       |              |       | <i>P</i> * |
|------------------------------------|-----------------|-------|--------------|-------|------------|
|                                    | Controls        |       | RLS patients |       |            |
|                                    | Mean            | ±SD   | Mean         | ±SD   |            |
| Dentate nucleus 25th <sup>#</sup>  | -0,172          | 0,033 | -0,165       | 0,024 | n.s.       |
| Dentate nucleus 50th <sup>#</sup>  | -0,060          | 0,027 | -0,062       | 0,022 | n.s.       |
| Red nucleus 25th <sup>#</sup>      | -0,265          | 0,055 | -0,234       | 0,056 | n.s.       |
| Red nucleus 50th <sup>#</sup>      | -0,141          | 0,039 | -0,132       | 0,043 | n.s.       |
| Substantia nigra 25th <sup>#</sup> | -0,287          | 0,046 | -0,243       | 0,077 | n.s.       |
| Substantia nigra 50th <sup>#</sup> | -0,138          | 0,042 | -0,119       | 0,072 | n.s.       |
| Basal ganglia 25th <sup>#</sup>    | -0,205          | 0,026 | -0,203       | 0,028 | n.s.       |
| Basal ganglia 50th <sup>#</sup>    | -0,075          | 0,015 | -0,081       | 0,016 | n.s.       |
| <b>Histogram of whole brain</b>    |                 |       |              |       |            |
| 10 <sup>th</sup> percentile        | -0,220          | 0,007 | -0,208       | 0,010 | 0.01       |
| 50 <sup>th</sup> percentile        | 0,000           | 0,003 | 0,002        | 0,001 | n.s.       |
| 90 <sup>th</sup> percentile        | 0,214           | 0,009 | 0,200        | 0,009 | 0.02       |

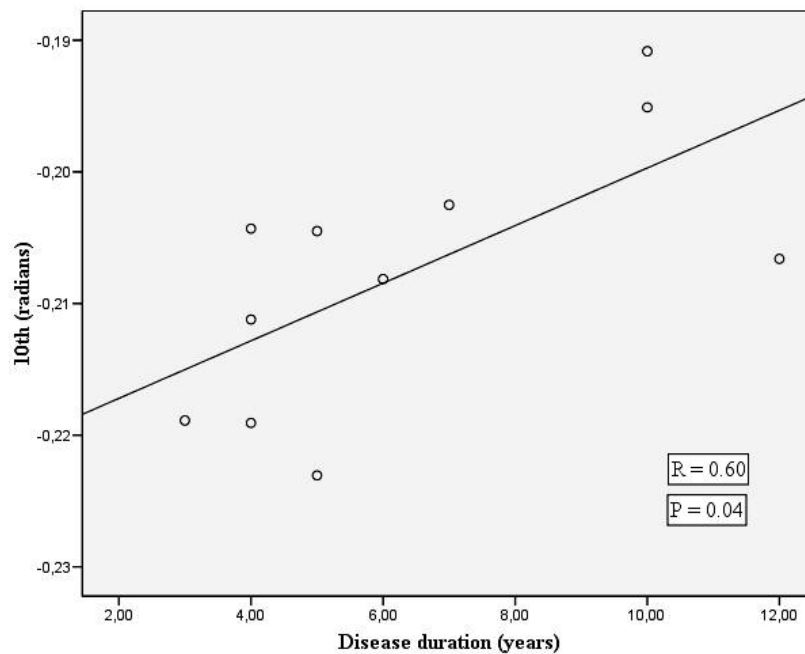
\*Mann–Whitney *U* test (a *P* value of < 0.05 after correction for multiple comparisons was considered to be significant). <sup>#</sup> = Mean of the left and right values.

**Figure 16.** Box-plots of 10<sup>th</sup>, 50<sup>th</sup> and 90<sup>th</sup> values from histograms of phase in RLS patients and controls.



\*\*=P<0.05

**Figure 17.** Correlation between 10<sup>th</sup> values from histograms of phase in RLS patients and disease duration (Spearman rank test).



## **REFERENCES**

- Accili D, Fishburn CS, Drago J, et al. A targeted mutation of the D3 dopamine receptor gene is associated with hyperactivity in mice. *Proc Natl Acad Sci USA* 1996;93:1945–1949.
- Agosta F, Rocca MA, Valsasina P, Sala S, Caputo D, Perini M, Salvi F, Prella A, Filippi M. A longitudinal diffusion tensor MRI study of the cervical cord and brain in amyotrophic lateral sclerosis patients. *J Neurol Neurosurg Psychiatry*. 2009;80:53-5.
- Allen RP, Earley CJ. Defining the phenotype of the restless legs syndrome (RLS) using age-of-symptom-onset. *Sleep Med* 2000;1:11-19.
- Allen RP, Barker PB, Wehrl F, Song HK, Earley CJ. MRI measurement of brain iron in patients with restless legs syndrome. *Neurology*. 2001;56:263-5.
- Allen RP, Picchiatti D, Hening WA, Trenkwalder C, Walters AS, Montplaisi J. Restless legs syndrome: diagnostic criteria, special considerations, and epidemiology. A report from the restless legs syndrome diagnosis and epidemiology workshop at the National Institutes of Health. *Sleep Med* 2003;4:101–19.
- Allen RP. Dopamine and iron in the pathophysiology of restless legs syndrome (RLS). *Sleep Med*. 2004;5:385-91.
- Allen RP, Earley CJ. The role of iron in restless legs syndrome. *Mov Disord*. 2007;22 Suppl 18:S440-8.
- Allen RP, Connor JR, Hyland K, Earley CJ. Abnormally increased CSF 3-Ortho-methyldopa (3-OMD) in untreated restless legs syndrome (RLS) patients indicates more severe disease and possibly abnormally increased dopamine synthesis. *Sleep Med* 2008;10:123–8.
- Apkarian AV, Bushnell MC, Treede RD, Zubieta JK. Human brain mechanisms of pain perception and regulation in health and disease. *Eur J Pain*. 2005;9:463-84.

- Ashburner J, Friston K. Voxel-based morphometry - The methods. *NeuroImage* 2000. 11,805-821.
- Astrakas LG, Konitsiotis S, Margariti P, Tsouli S, Tzarouhi L, Argyropoulou MI. T2 relaxometry and fMRI of the brain in late-onset restless legs syndrome. *Neurology*. 2008;71:911-6.
- Bara-Jimenez W, Aksu M, Graham B, Sato S, Hallett M. Periodic limb movements in sleep: state-dependent excitability of the spinal flexor reflex. *Neurology* 2000; 54:1609-16.
- Barrière G, Cazalets JR, Bioulac B, Tison F, Ghorayeb I. The restless legs syndrome. *Prog Neurobiol*. 2005;77:139-65.
- Bassetti CL, Mauerhofer D, Gugger M, Mathis J, Hess CW. Restless legs syndrome: a clinical study of 55 patients. *Eur Neurol*. 2001;45:67-74.
- Battaglini M, Giorgio A, Stromillo ML, Bartolozzi ML, Guidi L, Federico A, De Stefano N. Voxel-wise assessment of progression of regional brain atrophy in relapsing-remitting multiple sclerosis. *J Neurol Sci*. 2009;282:55-60.
- Bonavita S, Di Salle F, Tedeschi G. Proton MRS in neurological disorders. *Eur J Radiol*. 1999;30:125-31.
- Brand A, Richter-Landsberg C, Leibfritz D. Multinuclear NMR studies on the energy metabolism of glial and neuronal cells. *Dev Neurosci* 1993;15:289-98.
- Briellmann RS, Rosler KM, Hess CW. Blink reflex excitability is abnormal in patients with periodic leg movements in sleep. *Mov Disord* 1996;11:710 -14.
- Bucher SF, Seelos KC, Oertel WH, Reiser M, Trenkwalder C. Cerebral generators involved in the pathogenesis of the restless legs syndrome. *Ann Neurol* 1997;41:639-45.
- Celle S, Roche F, Peyron R, Faillenot I, Laurent B, Pichot V, Barthélémy JC, Sforza E. Lack of specific gray matter alterations in

restless legs syndrome in elderly subjects. *J Neurol*. 2009 Sep 22. [Epub ahead of print]

- Cervenka S, Pålhagen SE, Comley RA, Panagiotidis G, Cselényi Z, Matthews JC, Lai RY, Halldin C, Farde L. Support for dopaminergic hypoactivity in restless legs syndrome: a PET study on D2-receptor binding. *Brain*. 2006;129:2017-28.
- Clardy SL, Earley CJ, Allen RP, Beard JL, Connor JR. Ferritin subunits in CSF are decreased in restless legs syndrome. *J Lab Clin Med* 2006a;147:67 –73.
- Clardy SL, Wang X, Boyer PJ, Earley CJ, Allen RP, Connor JR. Is ferroportin-hepcidin signaling altered in restless legs syndrome? *J Neurol Sci*. 2006b;247:173-9.
- Clemens S, Rye D, Hochman S. Restless legs syndrome: revisiting the dopamine hypothesis from the spinal cord perspective. *Neurology*. 2006;67:125-30.
- Connor JR, Boyer PJ, Menzies SL, Dellinger B, Allen RP, Ondo WG, Earley CJ. Neuropathological examination suggests impaired brain iron acquisition in restless legs syndrome. *Neurology*. 2003;61:304-9.
- Connor JR, Wang XS, Patton SM, Menzies SL, Troncoso JC, Earley CJ, Allen RP. Decreased transferrin receptor expression by neuromelanin cells in restless legs syndrome. *Neurology*. 2004;62:1563-7.
- Connor JR, Wang XS, Allen RP, Beard JL, Wiesinger JA, Felt BT, Earley CJ. Altered dopaminergic profile in the putamen and substantia nigra in restless leg syndrome. *Brain*. 2009;132:2403-12.
- Corson PW, Nopoulos P, Miller DD, Arndt S, Andreasen NC. Change in basal ganglia volume over 2 years in patients with schizophrenia: typical versus atypical neuroleptics. *Am J Psychiatry* 1999;156:1200-4.

- Dean T Jr, Allen RP, O'Donnell CP, Earley CJ. The effects of dietary iron deprivation on murine circadian sleep architecture. *Sleep Med.* 2006;7:634-40.
- Desai AV, Cherkas LF, Spector TD, Williams AJ. Genetic influences in self-reported symptoms of obstructive sleep apnoea and restless legs: a twin study. *Twin Res* 2004; 7: 589–95.
- Dhawan V, Ali M, Chaudhuri KR. Genetic aspects of restless legs syndrome. *Postgrad Med J.* 2006;82:626-9.
- Earley CJ, Heckler D, Allen RP. Repeated IV doses of iron provides effective supplemental treatment of restless legs syndrome. *Sleep Med.* 2005;6:301-5.
- Earley CJ, Barker P, Horska A, Allen RP. MRI-determined regional brain iron concentrations in early- and late-onset restless legs syndrome. *Sleep Med.* 2006;7:458-61.
- Earley CJ, Ponnuru P, Wang X, Patton SM, Conner JR, Beard JL, Taub DD, Allen RP. Altered iron metabolism in lymphocytes from subjects with restless legs syndrome. *Sleep.* 2008;31:847-52.
- Earley CJ, Allen RP, Connor JR, Ferrucci L, Troncoso J. The dopaminergic neurons of the A11 system in RLS autopsy brains appear normal. *Sleep Med.* 2009;10:1155-7.
- Ekblom KA. Restless legs. *Acta Med Scand Suppl* 1945;158:5-123.
- Etgen T, Draganski B, Ilg C, Schroder M, Geisler P, Hajak G, Eisele I, Sander D, May A. Bilateral thalamic gray matter changes in patients with restless legs syndrome. *Neuroimage.* 2005;24:1242-7.
- Freeman A, Ciliax B, Bakay R, Daley J, Miller RD, Keating G, Levey A, Rye D. Nigrostriatal collaterals to thalamus degenerate in parkinsonian animal models. *Ann Neurol* 2001;50:321-9.
- Godau J, Klose U, Di Santo A, Schweitzer K, Berg D. Multiregional brain iron deficiency in restless legs syndrome. *Mov Disord.* 2008;23:1184-7.

- Good CD, Johnsrude IS, Ashburner J, Henson RN, Friston KJ, Frackowiak RS. A voxel-based morphometric study of ageing in 465 normal adult human brains. *Neuroimage* 2001;14:21-36
- Gosler A, Liepert J. Influence of Carbergoline on motor excitability in patients with restless legs syndrome. *J Clin Neurophysiol* 2007;24:456–60.
- Haacke EM, Cheng NY, House MJ, Liu Q, Neelavalli J, Ogg RJ, Khan A, Ayaz M, Kirsch W, Obenaus A. Imaging iron stores in the brain using magnetic resonance imaging. *Magn Reson Imaging*. 2005;23:1-25.
- Haacke EM, Mittal S, Wu Z, Neelavalli J, Cheng YC. Susceptibility-weighted imaging: technical aspects and clinical applications, part 1. *AJNR Am J Neuroradiol*. 2009;30:19-30.
- Hajek M, Dezortova M. Introduction to clinical in vivo MR spectroscopy. *Eur J Radiol*. 2008;67:185-93.
- Haselgrove JC, Moore JR. Correction for distortion of echo-planar images used to calculate the apparent diffusion coefficient. *Magn Reson Med* 1996;36:960-964.
- Hening WA, Allen RP, Washburn M, Lesage SR, Earley CJ. The four diagnostic criteria for Restless Legs Syndrome are unable to exclude confounding conditions ("mimics"). *Sleep Med*. 2009;10:976-81.
- Hilker R, Burghaus L, Razai N, Jacobs AH, Szelies B, Heiss WD. Functional brain imaging in combined motor and sleep disorders. *J Neurol Sci*. 2006;248:223-6.
- Hornyak M, Ahrendts JC, Spiegelhalder K, Riemann D, Voderholzer U, Feige B, van Elst LT. Voxel-based morphometry in unmedicated patients with restless legs syndrome. *Sleep Med*. 2007;9:22-6.

- Hue GE, Decker MJ, Solomon IG, Rye DB. Increased wakefulness and hyper-responsivity to novel environments in mice lacking functional dopamine D3 receptors. *Soc Neurosci* 2003;616:16.
- Jenkinson M, Bannister P, Brady M, Smith S. Improved optimization for the robust and accurate linear registration and motion correction of brain images. *Neuroimage*. 2002;17:825-41.
- Kantarci K, Knopman DS, Dickson DW, Parisi JE, Whitwell JL, Weigand SD et al. Alzheimer disease: postmortem neuropathologic correlates of antemortem <sup>1</sup>H MR spectroscopy metabolite measurements. *Radiology* 2008;248:210-20.
- Kutukcu Y, Dogruer E, Yetkin S, Ozgen F, Vural O, Aydin H. Evaluation of periodic leg movements and associated transcranial magnetic stimulation parameters in restless legs syndrome. *Muscle Nerve* 2006;33:133–7.
- Lazzarini A, Walters AS, Hickey K et al. Studies of penetrance and anticipation in five autosomal-dominant restless legs syndrome pedigrees. *Mov Disord* 1999; 14: 111–6.
- Lee SJ, Kim JS, Song IU, An JY, Kim YI, Lee KS. Poststroke restless legs syndrome and lesion location: anatomical considerations. *Mov Disord*. 2009;24:77-84.
- Levchenko A, Montplaisir JY, Asselin G et al. Autosomal-Dominant Locus for Restless Legs Syndrome in French-Canadians on Chromosome 16p12.1. *Mov Disord* 2009; 24(1):40-50.
- Lodi R, Parchi P, Tonon C, Manners D, Capellari S, Strammiello R, Rinaldi R, Testa C, Malucelli E, Mostacci B, Rizzo G, Pierangeli G, Cortelli P, Montagna P, Barbiroli B. Magnetic resonance diagnostic markers in clinically sporadic prion disease: a combined brain magnetic resonance imaging and spectroscopy study. *Brain*. 2009;132:2669-79.

- Lugaresi E, Coccagna G, Tassinari CA, Ambrosetto C. Polygraphic data on motor phenomena in the restless legs syndrome. *Riv Neurol.* 1965 Nov-Dec;35(6):550-61.
- Martinelli P, Rizzo G, Manners D, Tonon C, Pizza F, Testa C, Scaglione C, Barbiroli B, Lodi R. Diffusion-weighted imaging study of patients with essential tremor. *Mov Disord.* 2007;22:1182-5.
- Manconi M, Rocca MA, Ferini-Strambi L, Tortorella P, Agosta F, Comi G, Filippi M. Restless legs syndrome is a common finding in multiple sclerosis and correlates with cervical cord damage. *Mult Scler.* 2008;14:86-93.
- Martinelli P and Coccagna G. Rilievi neurofisiologici sulla sindrome delle gambe senza riposo. *Riv Neurol (Roma)* 1976; 46:552-560.
- Mascalchi M, Filippi M, Floris R, Fonda C, Gasparotti R, Villari N. Diffusion-weighted MR of the brain: methodology and clinical application. *Radiol Med.* 2005;109:155-97.
- Michaud M, Lavigne G, Desautels A, et al. Effects of immobility on sensory and motor symptoms of restless legs syndrome. *Mov Disord* 2002;17:112–5.
- Mignot E. A step forward for restless legs syndrome. *Nat Genet.* 2007;39:938-9.
- Montplaisir J, Boucher S, Nicolas A, et al. Immobilization tests and periodic leg movements in sleep for the diagnosis of restless leg syndrome. *Mov Disord* 1998;13:324–9.
- Möller JC, Unger M, Stiasny-Kolster K, Oertel WH. Restless Legs Syndrome (RLS) and Parkinson's disease (PD)-related disorders or different entities? *J Neurol Sci.* 2010;289:135-7.
- Nardone R, Ausserer H, Bratti A, et al. Cabergoline reverses cortical hyperexcitability in patients with restless legs syndrome. *Acta Neurol Scand* 2006;114:244–9.
- Nicolas A, Michaud M, Lavigne G, Montplaisir J. The influence of sex, age and sleep/wake state on characteristics of periodic leg

- movements in restless legs syndrome patients. *Clin Neurophysiol* 1999;110:1168–74.
- Nordlander NB. The therapy in restless legs. *Acta Med Scand* 1953;143:453–7.
  - Ogg RJ, Langston JW, Haacke EM, Steen RG, Taylor JS. The correlation between phase shifts in gradient-echo MR images and regional brain iron concentration. *Magn Reson Imaging*. 1999;17:1141-8.
  - Ondo WG, He Y, Rajasekaran S, Le WD. Clinical correlates of 6-hydroxydopamine injections into A11 dopaminergic neurons in rats: a possible model for restless legs syndrome. *Mov Disord*. 2000;15:154-8.
  - Oppenheim H. *Lehrbuch der Nervenkrankheiten*. 7th ed. Berlin, Germany: S Karger, 1923:1744.
  - Pierpaoli C, Jezzard P, Basser PJ, Barnett A, Di Chiro G. Diffusion tensor MR imaging of the human brain. *Radiology* 1996;201:637-648
  - Price DD. Psychological and neural mechanisms of the affective dimension of pain. *Science* 2000; 288:1769-72.
  - Provencher SW. Estimation of metabolite concentrations from localized in vivo proton NMR spectra. *Magn Reson Med* 1993;30: 672-9.
  - Qu S, Ondo WG, Zhang X, Xie WJ, Pan TH, Le WD. Projections of diencephalic dopamine neurons into the spinal cord in mice. *Exp Brain Res* 2006;168:152–156.
  - Qu S, Le W, Zhang X, Xie W, Zhang A, Ondo WG. Locomotion is increased in A11-lesioned mice with iron deprivation: a possible animal model for restless legs syndrome. *J Neuropathol Exp Neurol*. 2007;66:383-8.
  - Rye DB. Parkinson's disease and RLS: the dopaminergic bridge. *Sleep Med*. 2004;5:317-28.

- Rijsman RM, Stam CJ, Weerd AW. Abnormal H-reflexes in periodic limb movement disorder; impact on understanding the pathophysiology of the disorder. *Clin Neurophysiol* 2005;116:204-10.
- Rizzo G, Martinelli P, Manners D, Scaglione C, Tonon C, Cortelli P, Malucelli E, Capellari S, Testa C, Parchi P, Montagna P, Barbiroli B, Lodi R. Diffusion-weighted brain imaging study of patients with clinical diagnosis of corticobasal degeneration, progressive supranuclear palsy and Parkinson's disease. *Brain*. 2008;131:2690-700.
- Rizzo V, Aricò I, Mastroeni C, Morgante F, Giovanna L, Girlanda P, Silvestri R, Quartarone A. Dopamine agonists restore cortical plasticity in patients with idiopathic restless legs syndrome. *Mov Disord*. 2009;24:710-5.
- Rueckert D, Sonoda LI, Hayes C, Hill DL, Leach MO, Hawkes DJ. Nonrigid registration using free-form deformations: application to breast MR images. *IEEE Trans Med Imaging*. 1999;18:712-21.
- San Pedro EC, Mountz JM, Mountz JD, Liu HG, Katholi CR, Deutsch G. Familial painful restless legs syndrome correlates with pain dependent variation of blood flow to the caudate, thalamus, and anterior cingulated gyrus. *J Rheumatol* 1998;25:2270-5.
- Schattschneider J, Bode A, Wasner G, Binder A, Deuschl G, Baron R. Idiopathic restless legs syndrome: abnormalities in central somatosensory processing. *J Neurol*. 2004;251:977-82.
- Schmidauer C, Sojer M, Seppi K, Stockner H, Högl B, Biedermann B, Brandauer E, Peralta CM, Wenning GK, Poewe W. Transcranial ultrasound shows nigral hypoechogenicity in restless legs syndrome. *Ann Neurol*. 2005;58:630-4.
- Skagerberg G, Bjorklund A, Lindvall O, Schmidt RH. Origin and termination of the diencephalo-spinal dopamine system in the rat. *Brain Res Bull* 1982;9:237-244.

- Skagerberg G, Lindvall O. Organization of diencephalic dopamine neurons projecting to the spinal cord in the rat. *Brain Res* 1985;342:340-351.
- Smith SM. Fast robust automated brain extraction. *Hum Brain Mapp*. 2002;17:143-55.
- Smith SM, Jenkinson M, Woolrich MW, Beckmann CF, Behrens TE, Johansen-Berg H, Bannister PR, De Luca M, Drobnjak I, Flitney DE, Niazy RK, Saunders J, Vickers J, Zhang Y, De Stefano N, Brady JM, Matthews PM. Advances in functional and structural MR image analysis and implementation as FSL. *Neuroimage*. 2004;23 Suppl 1:S208-19.
- Smith SM, Jenkinson M, Johansen-Berg H, Rueckert D, Nichols TE, Mackay CE, Watkins KE, Ciccarelli O, Cader MZ, Matthews PM, Behrens TE. Tract-based spatial statistics: voxelwise analysis of multi-subject diffusion data. *Neuroimage*. 2006;31:1487-505.
- Smith SM, Johansen-Berg H, Jenkinson M, Rueckert D, Nichols TE, Miller KL, Robson MD, Jones DK, Klein JC, Bartsch AJ, Behrens TE. Acquisition and voxelwise analysis of multi-subject diffusion data with tract-based spatial statistics. *Nat Protoc*. 2007;2:499-503.
- Snyder AM, Wang X, Patton SM, Arosio P, Levi S, Earley CJ, Allen RP, Connor JR. Mitochondrial ferritin in the substantia nigra in restless legs syndrome. *J Neuropathol Exp Neurol*. 2009;68:1193-9.
- Stefansson H, Rye DB, Hicks A, Petursson H, Ingason A, Thorgeirsson TE, Palsson S, Sigmundsson T, Sigurdsson AP, Eiriksdottir I, Soebeck E, Bliwise D, Beck JM, Rosen A, Waddy S, Trotti LM, Iranzo A, Thambisetty M, Hardarson GA, Kristjansson K, Gudmundsson LJ, Thorsteinsdottir U, Kong A, Gulcher JR, Gudbjartsson D, Stefansson K. A genetic risk factor for periodic limb movements in sleep. *N Engl J Med*. 2007;357:639-47.

- Stiasny-Kolster K, Magerl W, Oertel WH, Moller JC, Treede RD. Static mechanical hyperalgesia without dynamic tactile allodynia in patients with restless legs syndrome. *Brain* 2004;127:773-82.
- Symonds CP. Nocturnal myoclonus. *J Neurol Neurosurg Psychiatry* 1953;16:166-71.
- Treede RD, Kenshalo DR, Gracely RH, Jones AK. The cortical representation of pain. *Pain* 1999;79:105-11.
- Trenkwalder C, Bucher SF, Oertel WH, et al. Bereitschaftspotential in idiopathic and symptomatic restless legs syndrome. *Electroencephalogr Clin Neurophysiol* 1993;89:95-103.
- Trenkwalder C, Bucher SF, Oertel WH. Electrophysiological pattern of involuntary limb movements in the restless legs syndrome. *Muscle Nerve* 1996;19:155-62.
- Trenkwalder C, Högl B and Winkelmann J. Recent advances in the diagnosis, genetics and treatment of restless legs syndrome. *J Neurol* 2009; 256(4):539-553.
- Trenkwalder C, Paulus W, Walters AS. The restless legs syndrome. *Lancet Neurol.* 2005;4:465-75.
- Trenkwalder C, Seidel VC, Gasser T, Oertel WH. Clinical symptoms and possible anticipation in a large kindred of familial restless legs syndrome. *Mov Disord* 1996; 11: 389–94.
- Tyvaert L, Houdayer E, Devanne H, Bourriez JL, Derambure P, Monaca C. Cortical involvement in the sensory and motor symptoms of primary restless legs syndrome. *Sleep Med.* 2009a;10:1090-6.
- Tyvaert L, Laureau E, Hurtevent JP, Hurtevent JF, Derambure P, Monaca C. A-delta and C-fibres function in primary restless legs syndrome. *Neurophysiol Clin.* 2009b;39:267-74.
- Unrath A, Kassubek J. Symptomatic restless leg syndrome after lacunar stroke: a lesion study. *Mov Disord.* 2006;21:2027-8.

- Unrath A, Juengling FD, Schork M, Kassubek J. Cortical grey matter alterations in idiopathic restless legs syndrome: An optimized voxel-based morphometry study. *Mov Disord.* 2007;22:1751-6.
- Unrath A, Müller HP, Ludolph AC, Riecker A, Kassubek J. Cerebral white matter alterations in idiopathic restless legs syndrome, as measured by diffusion tensor imaging. *Mov Disord.* 2008;23:1250-5.
- von Spiczak S, Whone AL, Hammers A, Asselin MC, Turkheimer F, Tings T, Happe S, Paulus W, Trenkwalder C, Brooks DJ. The role of opioids in restless legs syndrome: an [11C]diprenorphine PET study. *Brain.* 2005;128:906-17.
- Walters AS, Hickey K, Maltzman J, et al. A questionnaire study of 138 patients with restless legs syndrome: the 'Night-Walkers' survey. *Neurology* 1996;46:92–5.
- Walters AS, LeBrocq C, Dhar A, Hening W, Rosen R, Allen RP, Trenkwalder C; International Restless Legs Syndrome Study Group. Validation of the International Restless Legs Syndrome Study group rating scale for restless legs syndrome. *Sleep Med* 2003.4,121– 132.
- Walters AS. Toward a better definition of the restless legs syndrome. The International Restless Legs Syndrome Study Group. *Mov Disord.* 1995;10:634-42.
- Wang J, O'Reilly B, Venkataraman R, Mysliwicz V, Mysliwicz A. Efficacy of oral iron in patients with restless legs syndrome and a low-normal ferritin: A randomized, double-blind, placebo-controlled study. *Sleep Med.* 2009;10:973-5.
- Willis T. *The London practice of physick.* 1st ed. London: Thomas Bassett and William Crooke, 1685:404.
- Wetter TC, Eisensehr I, Trenkwalder C. Functional neuroimaging studies in restless legs syndrome. *Sleep Med.* 2004;5:401-6.
- Winkelmann J, Wetter TC, Collado-Seidel V, Gasser T, Dichgans M, Yassouridis A, Trenkwalder C. Clinical characteristics and

frequency of the hereditary restless legs syndrome in a population of 300 patients. *Sleep* 2000; 23: 597–602.

- Winkelmann J, Muller-Myhsok B, Wittchen HU, Hock B, Prager M, Pfister H, Strohle A, Eisensehr I, Dichgans M, Gasser T, Trenkwalder C. Complex segregation analysis of restless legs syndrome provides evidence for an autosomal dominant mode of inheritance in early age at onset families. *Ann Neurol* 2002;52:297–302.
- Winkelmann J, Polo O, Provini F, Nevsimalova S, Kemlink D, Sonka K, Högl B, Poewe W, Stiasny-Kolster K, Oertel W, de Weerd A, Strambi LF, Zucconi M, Pramstaller PP, Arnulf I, Trenkwalder C, Klein C, Hadjigeorgiou GM, Happe S, Rye D, Montagna P. Genetics of restless legs syndrome (RLS): State-of-the-art and future directions. *Mov Disord.* 2007a;22 S18:S449-58.
- Winkelmann J, Schormair B, Lichtner P, Ripke S, Xiong L, Jalilzadeh S, Fulda S, Pütz B, Eckstein G, Hauk S, Trenkwalder C, Zimprich A, Stiasny-Kolster K, Oertel W, Bachmann CG, Paulus W, Peglau I, Eisensehr I, Montplaisir J, Turecki G, Rouleau G, Gieger C, Illig T, Wichmann HE, Holsboer F, Müller-Myhsok B, Meitinger T. Genome-wide association study of restless legs syndrome identifies common variants in three genomic regions. *Nat Genet* 2007b; 39:1000-1006.
- Wittmaack T. Pathologie und therapie der sensibilitat-neurosen. Leipzig: E. Schafer, 1861:459.
- Zhang Y, Brady M, Smith S. Segmentation of brain MR images through a hidden Markov random field model and the expectation-maximization algorithm. *IEEE Trans Med Imaging.* 2001;20:45-57.
- Zhao H, Zhu W, Pan T, Xie W, Zhang A, Ondo WG, Le W. Spinal cord dopamine receptor expression and function in mice with 6-OHDA lesion of the A11 nucleus and dietary iron deprivation. *J Neurosci Res.* 2007;85:1065-76.

- Zucconi M, Ferini-Strambi L. Epidemiology and clinical findings of restless legs syndrome. *Sleep Med.* 2004 May;5:293-9.
- Zucconi M, Ferri R, Allen R, Baier PC, Bruni O, Chokroverty S, Ferini-Strambi L, Fulda S, Garcia-Borreguero D, Hening WA, Hirshkowitz M, Högl B, Hornyak M, King M, Montagna P, Parrino L, Plazzi G, Terzano MG; International Restless Legs Syndrome Study Group (IRLSSG). The official World Association of Sleep Medicine (WASM) standards for recording and scoring periodic leg movements in sleep (PLMS) and wakefulness (PLMW) developed in collaboration with a task force from the International Restless Legs Syndrome Study Group (IRLSSG). *Sleep Med.* 2006;7:175-83.

Thanks to:

Prof. Pasquale Montagna, Prof. Raffaele Lodi, Dott. David Manners, Prof. Paolo Martinelli, Prof. Bruno Barbiroli, Dott. Roberto Vetrugno, Prof.ssa Caterina Tonon, Dott.ssa Sara Marconi, Dott.ssa Claudia Testa, Dott. Fabio Pizza, Dott. Emil Malucelli, Dott. Giuseppe Plazzi, Dott.ssa Federica Provini, Dott.ssa Cesa Scaglione, Dott.ssa Giovanna Calandra-Bonaura, Dott. Pietro Guaraldi, Dott.ssa Ilaria Naldi, Dott.ssa Francesca Poli.